

BLOOD FLOW DYNAMICS IN MICROVESSEL BIFURCATIONS

MOHAMAD THARMIZI BIN MOHAMAD EHSAN

Thesis submitted is fulfilled of requirement
for the award of degree of
Bachelor of Mechanical Engineering

Faculty of mechanical engineering
UNIVERSITY MALAYSIA PAHANG

November 2009

SUPERVISOR'S DECLARATION

I hereby declare that I have checked this project and in my opinion, this project is adequate in terms of scope and quality for the award of the degree of Bachelor of Mechanical Engineering.

Signature

Name of Supervisor: MOHAMAD MAZWAN BIN MAHAT

Position: LECTURER

Date: 24 NOVEMBER 2009

STUDENT'S DECLARATION

I hereby declare that the work in this project is my own except for quotations and summaries which have been duly acknowledged. The project has not been accepted for any degree and is not concurrently submitted for award of other degree.

Signature

Name: MOHAMAD THARMIZI BIN MOHAMAD EHSAN

ID Number: MA06055

Date: 24 NOVEMBER 2009

Dedicated to my parents

ACKNOWLEDGEMENTS

I am grateful and would like to express my sincere gratitude to my supervisor Mr Mohamad Mazwan Bin Mahat for his germinal ideas, invaluable guidance, continuous encouragement and constant support in making this research possible. He has always impressed me with his outstanding professional conduct, his strong conviction for science, and his belief that a degree program is only a start of a life-long learning experience. I appreciate his consistent support from the first day I applied to graduate program to these concluding moments. I am truly grateful for his progressive vision about my training in science, his tolerance of my naïve mistakes, and his commitment to my future career. I also sincerely thanks for the time spent proof reading and correcting my many mistakes.

My sincere thanks go to all my labmates and members of the staff of the Mechanical Engineering Department, UMP, who helped me in many ways and made my stay at UMP pleasant and unforgettable. Many special thanks go to member in my group research with the same supervisor for their excellent co-operation, inspirations and supports during this study.

I acknowledge my sincere indebtedness and gratitude to my parents for their love, dream and sacrifice throughout my life. I am also grateful to my fiance for her sacrifice, patience, and understanding that were inevitable to make this work possible. I cannot find the appropriate words that could properly describe my appreciation for their devotion, support and faith in my ability to attain my goals. Special thanks should be given to my committee members. I would like to acknowledge their comments and suggestions, which was crucial for the successful completion of this study.

ABSTRACT

This thesis deals with the blood flow behaviour in the microvessel bifurcation using variety of blood parameters. There are two situations for the analysis which normal microvessel and abnormal microvessel bifurcations. The objectives of this thesis are to investigate the effect of bifurcation on blood flow distributions and predict flow abnormalities due to blood properties. The thesis describes the finite volume technique to predict the abnormalities and identify the effect of the bifurcation. The structural three-dimensional solid modeling of normal and abnormal blood vessel were developed using the computer-aided drawing software. The strategy of validation of finite volume model was developed. The finite volume analysis was then performed using COSMOS Flow in Solidwork software. From the result, it is observed that bifurcation give an effect to the blood flow behavior. For normal and abnormal case, using the different pressure for same diameter of blood vessel bifurcation, the pressure result shown an increment when blood flow into the bifurcation. It is same when analyze using different velocity for same diameter, the value will decrease when it goes to the bifurcation. For analysis using different diameter of blood vessel bifurcation, the effect of bifurcation will clearly seen. Pressure and velocity will be proportional in values of analysis refer to the equation of fluid dynamics. Peak velocity of the normal and abnormal also showed different values. Normal microvessel bifurcation has a higher value of peak velocity than abnormal microvessel bifurcation. Reynolds Number also get an effect when the diameter of the blood vessel increase. Finally, the correlations obtained from this numerical result could be used to investigate the pressure and velocity distribution around the diseased segment.

ABSTRAK

Tesis ini membentangkan tentang sifat darah pada salur darah yang bercabang dua menggunakan parameter darah yang berbeza. Terdapat dua situasi di dalam analisis ini iaitu salur darah bercabang normal dan juga salur darah bercabang tidak normal. Objektif tesis ini ialah untuk mengenalpasti kesan salur darah bercabang kepada pergerakan darah dan untuk menjangka pergerakan darah tidak normal berdasarkan sifat darah itu sendiri. Tesis ini membincangkan penilaian kebolehtahanan untuk menjangka sesuatu tidak normal dalam salur darah dan kesan cabang pada pergerakan serta sifat darah. Permodelan struktur tiga dimensi untuk salur darah normal dan tidak normal dibangunkan dengan perisian lukisan bantuan komputer. Strategi pengesahan model kelantangan terhingga dibangunkan. Analisis kelantangan terhingga dijalankan dengan COSMOS di dalam perisian Solidwork. Keputusan yang diperolehi daripada analisis ialah cabang pada salur darah memberi kesan kepada pergerakan dan sifat darah. Bagi kes salur darah normal dan tidak normal menggunakan tekanan yang berbeza tetapi diameter sama, nilai tekanan menunjukkan peningkatan apabila darah melalui cabang. Ia juga sama apabila analisis kelajuan darah berbeza pada diameter yang sama, ia menunjukkan penurunan apabila sampai ke salur darah yang bercabang. Bagi analisis untuk diameter salur darah yang berbeza, kesan disebabkan salur darah bercabang dapat kelihatan dengan jelas. Tekanan dan kelajuan adalah bertentangan antara satu sama lain merujuk kepada persamaan dalam dinamik berdalir. Kelajuan tertinggi darah turut memberi nilai yang berbeza dalam kes salur darah normal dan tidak normal. Salur darah normal mempunyai nilai kelajuan tertinggi lebih daripada salur darah tidak normal. Nombor Reynold juga menunjukkan kesan apabila diameter salur darah berubah. Perkaitan diperolehi daripada kajian ini boleh dimanfaatkan untuk lanjutan taburan tekanan dan kelajuan bagi darah disekitar tempat yang sakit.

TABLE OF CONTENTS

SUPERVISOR’S DECLARATION	ii	
STUDENT’S DECLARATION	iii	
DEDICATION	iv	
ACKNOWLEDGEMENTS	v	
ABSTRACT	vi	
ABSTRAK	vii	
TABLE OF CONTENTS	viii	
LIST OF TABLES	xi	
LIST OF FIGURES	xii	
LIST OF SYMBOLS	xv	
LIST OF ABBREVIATIONS	xvi	
CHAPTER 1 : INTRODUCTION		
1.1	Background	1
1.2	Blood	2
1.3	Blood vessel	3
	1.3.1 Blood vessel disease	3
	1.3.1.1 Signs of blood vessel disease	3
	1.3.1.2 Risk factors	4
1.4	Blood flow profile at the branches	8
1.5	Blood content	9
1.6	Blood flow profiles at arterial	11
1.7	Flow at the bifurcations	12
1.8	Objectives	16
1.9	Scopes	16

CHAPTER 2 : FLOW BEHAVIOR IN MICROVESSEL BIFURCATIONS

2.1	Flow behaviour in microvessel bifurcations	17
2.2	Flow in bifurcations	19
2.2.1	Coronary arterial flow	19
2.2.2	Cerebral arterial flow	22
2.2.3	carotid bifurcation	23
2.3	Concept and theory of bifurcation	27
2.4	Closure	29

CHAPTER 3 : METHODOLOGY

3.1	Geometry of model	30
3.2	Simulations assumption and parameter	31
3.3	Geometry of the model	31
3.4	Boundary condition	34
3.4.1	Initial velocity	35
3.5	Governing equation of blood flow	37
3.6	Finite volume method	38
3.7	Visualization of simulations	39

CHAPTER 4 : RESULTS AND DISCUSSIONS

4.1	Result	40
4.2	Velocity blood flow	41
4.3	Pressure blood flow	52
4.4	Reynold's number	58

CHAPTER 5 : CONCLUSION AND RECOMMENDATIONS

5.1 Conclusion 64

5.2 Recommendations 65

REFERENCES 66

APPENDICES

A Data collection for velocity 70

B Data collection for pressure 74

LIST OF TABLE

Table No		Page
1.1	Table of blood vessel disease	5
3.1	Parameter used in simulation	31
4.1	Peak velocity vs diameter	50
4.2	Peak velocity percentage vs diameter	51
4.3	Change of blood vessel diameter	58
4.4	Change velocity of the blood flow	59

LIST OF FIGURES

Figure No		Page
1.1	Pressure and velocity pulse waveforms of a dog	10
1.2	Flow velocity waveform in a normal femoral arterial flow	11
1.3	The velocity profiles for pulsatile flow in a rigid tube	11
1.4	Flow field represented by streamlines	12
1.5	Fluid flow in bifurcation design	15
2.1	Multi branched model of the human arterial system	18
2.2	The profiles during systole show no flow reversal at the flow divider	20
2.3	During diastole, the velocity profile is skewed toward the flow divider and develops a stair-step shape from the secondary flows	21
2.4	Streamlines indicating the complex flow inside the cerebral aneurysm	22
2.5	Dimension of carotid bifurcation	24
2.6	Effect on Newtonian fluid	25
2.7	Effect on non-Newtonian fluid	25
2.8	Graph for the Newtonian and non Newtonian fluid effect	25
2.9	Flow for result for pulsatile flow	26
2.10	Vortex carotid flow using fluent for $Re = 290$	26
2.11	Vortex carotid flow for $Re = 700$	27
2.12	Structures of bifurcations	27
3.1	Process in Computational Fluid Dynamics	30
3.2	Normal microvessel bifurcations models	32
3.3	Abnormal microvessel bifurcations model	33
3.4	The model geometry taken from literature	33

3.5	Graph of the blood velocity profile in common femoral artery	35
3.6	Pressure input for normal blood vessel model	36
3.7	Pressure input for abnormal blood vessel	36
3.8	Visualization of blood flow streamlines in normal microvessel	37
4.1	Velocity flow for normal microvessel bifurcations	42
4.2	Velocity flow for abnormal microvessel bifurcations	42
4.3	Graph velocity vs length for different velocity in normal case	43
4.4	Graph velocity vs length for different velocity in abnormal case	43
4.5	Graph velocity vs length for different diameter in normal case	44
4.6	Graph velocity vs length for different diameter in abnormal case	45
4.7	Velocity flow for normal blood vessel diameter 5mm	46
4.8	Velocity flow for normal blood vessel diameter 7mm	46
4.9	Velocity flow for normal blood vessel diameter 10mm	46
4.10	Velocity flow for normal blood vessel diameter 12mm	46
4.11	Velocity flow for normal blood vessel diameter 14mm	47
4.12	Velocity flow for abnormal blood vessel diameter 5mm	47
4.13	Velocity flow for abnormal blood vessel diameter 7mm	47
4.14	Velocity flow for abnormal blood vessel diameter 10mm	47
4.15	Velocity flow for abnormal blood vessel diameter 12mm	47
4.16	Velocity flow for abnormal blood vessel diameter 14mm	48
4.17	Graph peak velocity vs diameter for normal case	48
4.18	Graph peak velocity vs diameter for abnormal case	49
4.19	Graph percentage peak velocity different vs diameter	51
4.20	Graph pressure vs length for different velocity in normal case	52
4.21	Graph pressure vs length for different velocity in abnormal case	52

4.22	Graph pressure vs length for different diameter in normal case	53
4.23	Graph pressure vs length for different diameter in abnormal case	54
4.24	Pressure flow for normal microvessel bifurcations	55
4.25	Pressure flow for abnormal microvessel bifurcations	55
4.26	Pressure flow for normal blood vessel diameter 5mm	56
4.27	Pressure flow for normal blood vessel diameter 7mm	56
4.28	Pressure flow for normal blood vessel diameter 10mm	56
4.29	Pressure flow for normal blood vessel diameter 12mm	56
4.30	Pressure flow for normal blood vessel diameter 14mm	57
4.31	Pressure flow for abnormal blood vessel diameter 5mm	57
4.32	Pressure flow for abnormal blood vessel diameter 7mm	57
4.33	Pressure flow for abnormal blood vessel diameter 10mm	57
4.34	Pressure flow for abnormal blood vessel diameter 12mm	57
4.35	Pressure flow for abnormal blood vessel diameter 14mm	58
4.36	Graph Reynolds number vs diameter of blood vessel	59
4.37	Graph Reynolds number vs velocity of blood vessel	60

LIST OF SYMBOLS

- u_i : velocity in the i -th direction
- P : pressure
- f_i : body force
- μ_i : viscosity
- δ_{ij} : Kronocker delta
- ρ : density
- v : mean velocity
- D : diameter
- ∂t : partial differential of time
- ∂p : partial differential of pressure
- R : radius
- L : length
- α : alpha
- A : area
- V : volume

LIST OF ABBREVIATIONS

- MCA : Middle cerebral artery
- CFD : Computational Fluid Dynamics
- CAD : Computer Aided Design
- FEM : Finite Element Method
- CT : Computer-assisted tomography
- CAE : Computer Aided Engineering
- CSS : Computational Solid Stress
- FEA : Finite Element Analysis
- PDE : Partial Differential Equation

CHAPTER 1

INTRODUCTION

1.1 BACKGROUND

Currently many diseases have been detected by the doctor or researcher in the medical part. One of the main part in the body which mostly detected as the place to create a disease is at the micro vessel bifurcations. This micro vessel bifurcation is the place where the blood will be separated into two ways. The flow of the blood will going through the micro vessel bifurcations or as known as micro channel and sometimes something happen at that part. In our body have many micro channel especially in the lung, aorta, and brain. All this micro channel have a potential to be the reason why many disease happen in the body but we must thinking clearly that it must be have a reason on that.

This project concerns about the disease which can happen in the micro vessel bifurcation depend on the blood profile or parameter. What will happen if the pressure increases at that place or is the velocity of the blood will cause the disease at that part. In order to satisfy the main concern of this project, it will focus on the blood profile or parameter in the blood vessel and also at the micro vessel bifurcations. Currently many disease have been detected by the researcher in the medical field and also doctor at this part of blood vessel but still have unknown reason why it happen and how it can be like that. The results of this fluid dynamics analysis through numerical simulations are expected to

explain this problem and help the people in medical to search the best treatment for the disease.

1.2 BLOOD

Blood carries substances such as nutrients and oxygen to all body's cells and transport waste product away from those same cells. In vertebrates, the blood composed of blood cells suspended in a liquid called volume blood plasma. 55% of blood fluids content in plasma, 90% by volume mostly water, and contains dissolved proteins, glucose, mineral ions, hormones, carbon dioxide (plasma being the main medium for excretory product transportation), platelets and blood cells themselves. Blood cells have two types which are red blood cells and white blood cells, including leukocytes and platelets (also called thrombocytes). The most abundant cells in vertebrate blood are red blood cells. Hemoglobin, an iron containing protein, will help in increasing the transportation of blood oxygen by reversibly binding to this respiratory gas and increasing solubility in blood. Carbon dioxide will dissolved in plasma as bicarbonate ion for transport out the body. Vertebrate blood is bright-red when its hemoglobin is oxygenated.

Some animals use hemoglobin to carry oxygen, instead of hemoglobin such as crustaceans and mollusks. A fluid called hemolymph, have been used by insect and some mollusks instead of blood, the difference being that hemolymph is not contain in a closed circulatory system. Most insects use hemolymph does not contain oxygen-carrying molecules because of their size of their body is too small enough. Jawed vertebrates have an adaptive immune system, based largely on white blood cells. Infections and parasites will be resisting by white blood cells. Platelets are important in the clotting of blood. Hemolymphs which use by arthropods have hemocytes as their immune system. The pumping action by heart make the blood circulated around the body through blood vessels. Arterial blood in animal which have the lungs carries oxygen from inhaled air to the tissues of the body and venous blood carries carbon dioxide, a waste product of metabolism produced by cells, from the tissues to the lungs to be exhaled.

Blood performs many important functions within the body including supply oxygen to the tissues. It also supply of nutrients such as glucose, amino acids and fatty acids. Fatty acids dissolved in the blood or bound to plasma proteins for example blood lipids. Blood also function as removal of waste such as carbon dioxide, urea and lactic acid. Besides that, blood function as well as regulation of core body temperature. Then, it can be hydraulics functions in our body.

1.3 BLOOD VESSEL

These are the part of circulatory system that transports blood throughout the body. Blood vessel have three major types: arteries, the capillaries, which enable the actual exchange of water and chemicals between the blood and the tissues; and the veins, which carry blood from the capillaries back towards the heart.

1.3.1 Blood vessel disease

Peripheral vascular disease or artery disease is related to the blood vessel disease. This type of disease is about blood vessel in the abdomen, legs and arms. When the blood vessels narrow, less oxygen-rich blood gets to your body parts. This can cause tissue and cell death or gangrene. This disease is the leading cause of amputations. The cause of this disease appears when a build-up of fatty deposits called plaque. Otherwise, the blood vessel or blood clots can cause other problems.

1.3.1.1 Signs of Blood Vessel Disease

Blood vessel disease also have a sign to show that a person might get it. First, the person will have muscle pain, aches or cramps on their body. Second, they will get cool, pale skin, cold both of their hands and feet. Third, the symptom is the person will get reddish-blue colour of the skin and nails of the hands and feet. Other symptoms is a sore that takes a long time to heal or scabbed over. Then, they loss of their hair on legs, feet or toes. Lastly, they will get faint or no pulse in the legs or feet.

1.3.1.2 Risk factors

All human being will get the blood vessel disease if cannot keep body healthy. A person is at higher risk for blood vessel disease if they are smoking. This habit will make their lungs and also the blood vessel worst. People who have diabetes also get a high risk to get this blood vessel disease. Then, people who are over 45 and have high cholesterol and blood pressure also open with this disease. Other risk peoples to get this disease are people who are overweight and inactive.



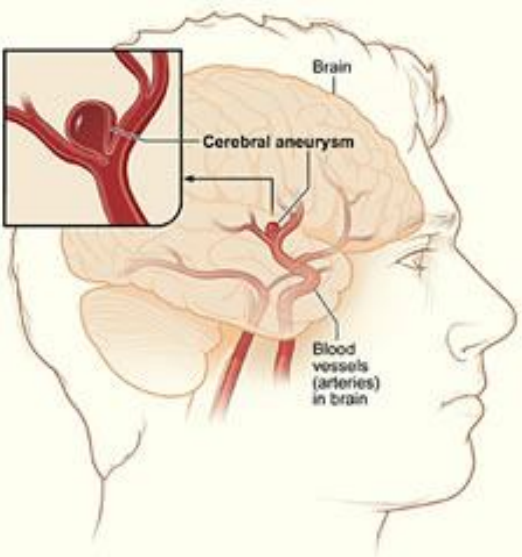
1.3.2 Anatomy

The arteries and veins have the same basic structure. There are three layers, from inside to outside while the capillaries have only one thick cell:

- *Tunica intima* (the thinnest layer): a single layer of simple squamous endothelial cells glued by a polysaccharide intercellular matrix, surrounded by a thin layer of sub endothelial connective tissue interlaced with a number of circularly arranged elastic bands called the *internal elastic lamina*.
- *Tunica media* (the thickest layer): circularly arranged elastic fiber, connective tissue, polysaccharide substances, the second and third layer are separated by another thick elastic band called external elastic lamina. The tunica media may (especially in arteries) be rich in vascular smooth muscle, which controls the caliber of the vessel.
- *Tunica adventitia*: entirely made of connective tissue. It also contains nerves that supply the muscular layer, as well as nutrient capillaries (*vasa vasorum*) in the larger blood vessels.

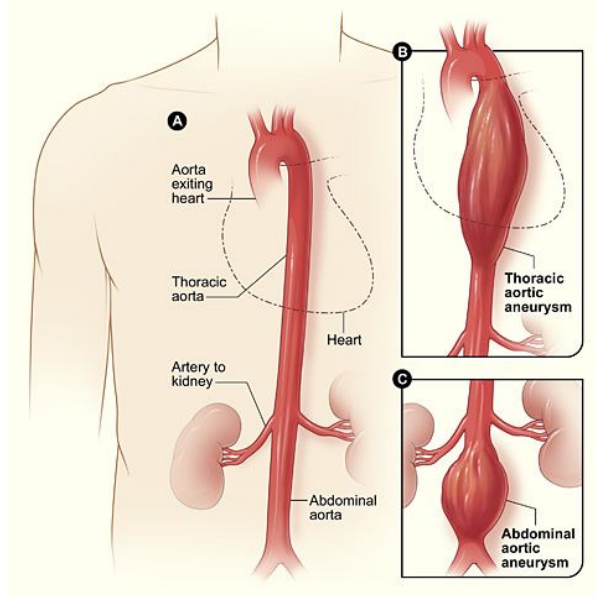
Capillaries consist of little more than a layer of endothelium and occasional connective tissue. When blood vessels connect to form a region of diffuse vascular supply it is called an anastomosis (pl. anastomoses). Anastomoses provide critical alternative routes for blood to flow in case of blockages. Laid end to end all the blood vessels in an average human body would encircle the earth twice, a distance of approximately 100,000 kilometers.

Table 1.1 Table of blood vessel diseases

Name of the disease	Picture
Aneurysm:	
a) Saccular aneurysm (Source: www.daviddarling.info)	
b) Fusiform aneurysm (Source: www.daviddarling.info)	
c) Cerebral aneurysm (Source: www.inventorspot.com)	

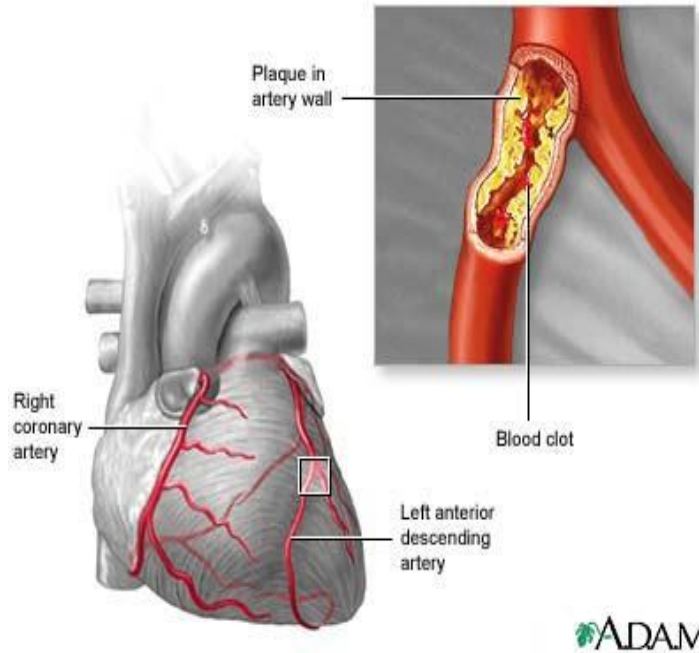
d)Aortic aneurysm

(Source:www.inventorspot.com)



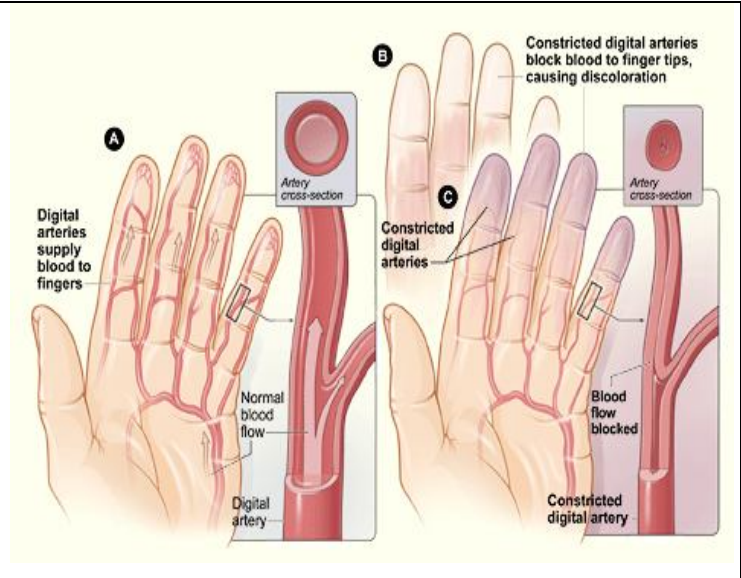
Coronary artery disease

(Source:www.adam.about.com)



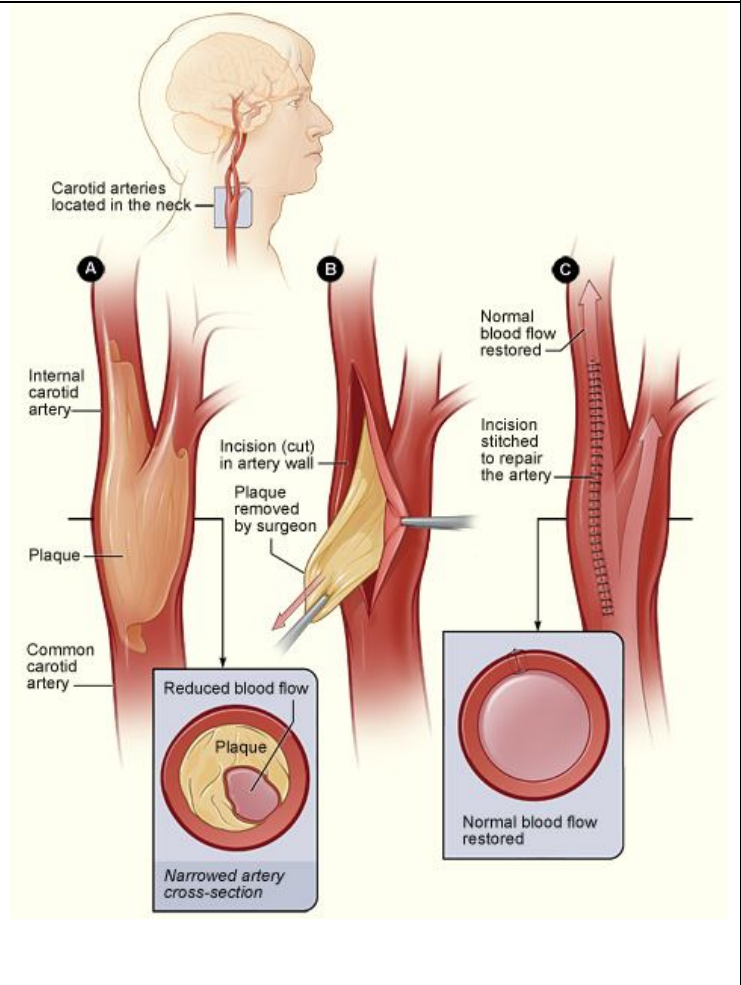
Raynauld disease

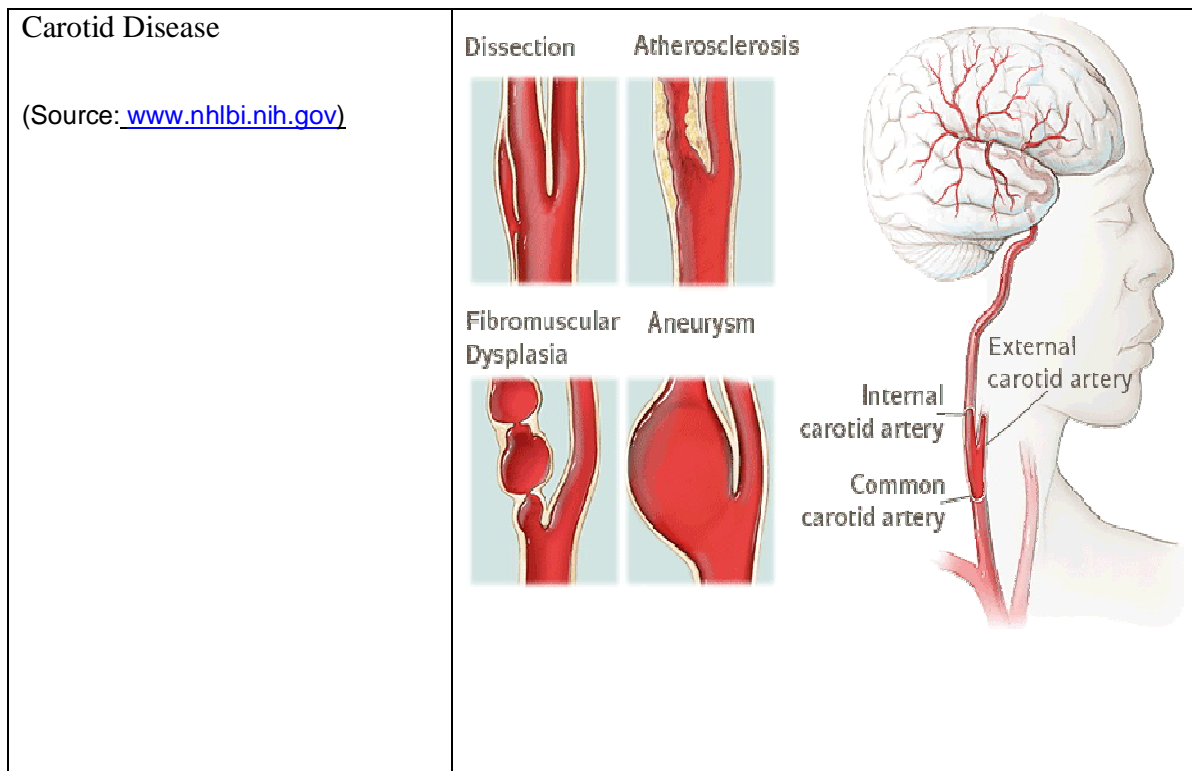
(Source: www.vascularweb.org)



Carotid disease

(Source: www.nhlbi.nih.gov)





1.4 BLOOD FLOW PROFILE AT THE BRANCHES

Blood flow in arteries is dominated by unsteady flow phenomena. A nondimensional frequency parameter, the Womersley number, governs the relationship between the unsteady and viscous forces. Normal arterial flow is laminar with secondary flows generated at curves and branches. The arteries are living organs that can adapt to and change with the varying hemodynamic conditions. In certain circumstances, unusual hemodynamic conditions create an abnormal biological response. Velocity profile skewing can create pockets in which the direction of the wall shear stress oscillates. Atherosclerotic disease tends to be localized in these sites and results in a narrowing of the artery lumen stenosis. The stenosis can cause turbulence and reduce flow by means of viscous head losses and flow choking. Very high shear stresses near the throat of the stenosis can activate platelets and thereby induce thrombosis, which can totally block blood flow to the heart or brain. Detection and quantification of stenosis serve as the basis for surgical intervention.

1.5 BLOOD CONTENTS

Blood is a complex mixture of cells, proteins, lipoproteins, and ions by which nutrients and wastes are transported. 40% of blood typically comprises approximately red blood cells by volume. Because red blood cells are small semisolid particles, they increase the viscosity of blood and affect the behavior of the fluid. Blood has four times more viscosity than water. Furthermore, blood does not exhibit a constant viscosity at all flow rates and is especially non-Newtonian in the microcirculatory system. When the red blood cells clump together into larger particles the non-Newtonian behavior is the most evident at a very low shear stress. Blood also exhibits non-Newtonian behavior in small branches and capillaries, where the cells squeeze through and a cell-free skimming layer reduces the effective viscosity through the tube.

However, in most arteries, blood will become a Newtonian fluid, and the viscosity can be taken as a constant, 4 centipoises. Non-Newtonian viscosity is extensively studied in the field of biorheology and has been reviewed by others (e.g. Chien 1970, Rodkiewicz et al 1990). Pressure and blood flow are unsteady. Heart pumps the blood with the cyclic nature of rotation creates periodic conditions in all arteries. Blood will be in and out from the heart by alternating cycles called *systole* and *diastole*. During systole, blood will be pumped out from the heart. Then, heart rests during diastole, and no blood is ejected.

Pressure and flow have characteristic pulsatile shapes that vary in different parts of the arterial system. Blood flow out of the heart is intermittent and will become zero when the aortic valve is closed. Aorta which is the largest artery in the human body also taking the large blood out of the heart, serves as a compliance chamber that provides a reservoir of high pressure during diastole as well as systole. Because of that, the blood pressure in most arteries is pulsatile, yet does not go to zero during diastole. In contrast, the flow is zero or even reversed during diastole in some arteries such as the external carotid, brachial, and femoral arteries. These arteries have a high downstream resistance during rest and the flow is essentially on or off with each cycle. In other arteries such as the internal carotid or

the renal arteries, the flow can be high during diastole if the downstream resistance is low. The flow in these arteries is more uniform.

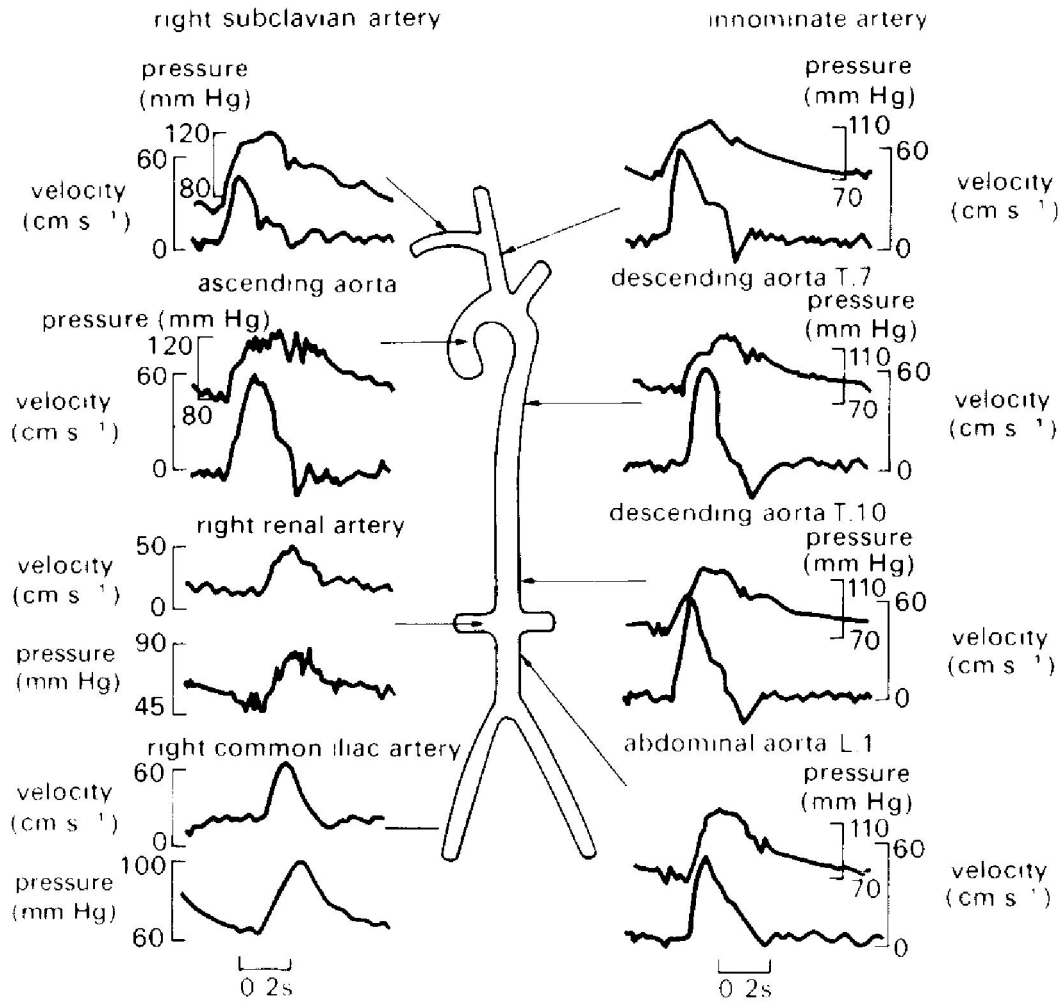


Figure 1.1 Pressure and velocity pulse waveforms of a dog

(Caro et al, 1978)

1.6 BLOOD FLOW PROFILE IN ARTERIALS

Vascular biologists are currently more concerned with the local hemodynamic conditions in a given artery or branch than simply the flow waveform predicted by IO models. A detailed local description of these pulsatile flows is needed. The fluid-wall shear stress in a blood vessel for a given pulsatile flow situation often needs to be determined. Fully developed pulsatile flow in a straight or tapered tube can be expressed analytically (Womersley 1955). A physiologic pressure or flow waveform can be expanded as a Fourier series, and the harmonic components of velocity can be summed to yield the unsteady velocity profiles.

Although in the past this summation was carried out by hand with tables, now it can be easily calculated using a simple computer program such as Mathematica (He et al 1993). Figure 3 shows an example of velocity profiles for a femoral artery of a dog. The Womersley solution for velocity can be used to generate excellent approximations for shear stress as long as secondary and separated flows are not present. Analytical solutions have also been obtained for flow through arteries that translate or change their radius of curvature, such as coronary arteries, which ride on the moving heart surface (Delfino et al 1994).

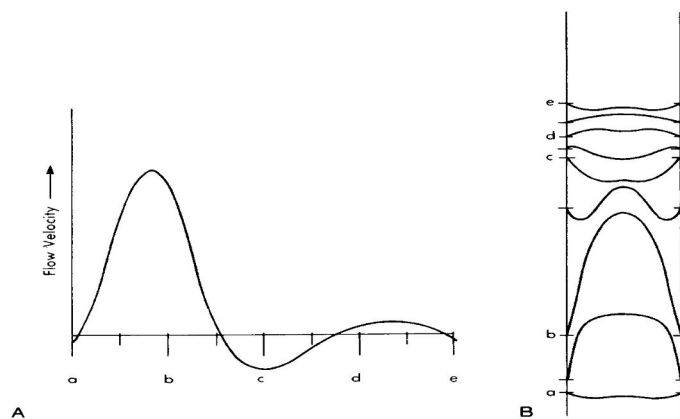


Figure 1.2 (A) Flow velocity waveform in a normal femoral arterial flow.

Figure 1.3 (B) The velocity profiles for pulsatile flow in a rigid tube

(W. B. Saunders, 1998)

1.7 FLOW AT THE BIFURCATIONS

We will focus our attention on the flow field represented by the streamlines of Figure 1.4. Let us consider a certain quantity of matter at sometime t enclosed by the solid line. At some later time $t + \Delta t$, the boundary of the system has a new physical location as represented by the dotted line.

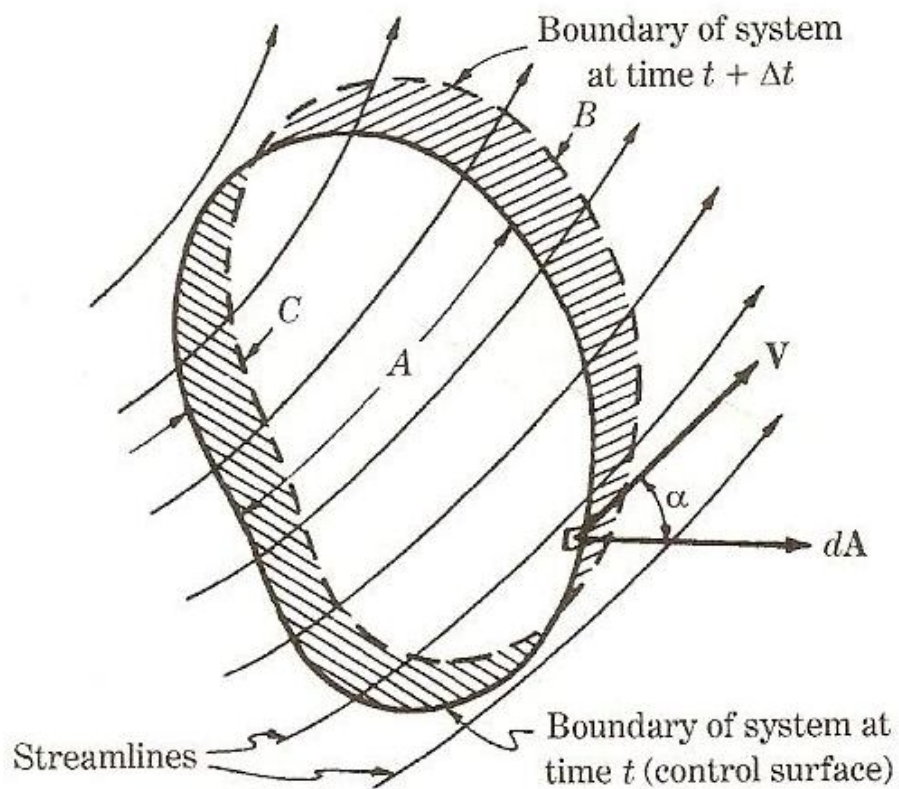


Figure 1.4 Flow field represented by streamlines

Considering the regions denoted by A, B and C, we have the system occupying the region A at the time t regions and different times with the appropriate subscripts,

$$m_A(t) = m_A(t + \Delta t) - m_C(t + \Delta t) + m_B(t + \Delta t) \quad (1.1)$$

Rearranging and dividing by Δt ,

$$\frac{m_A(t + \Delta t) - m_A(t)}{\Delta t} - \frac{m_B(t + \Delta t) - m_C(t + \Delta t)}{\Delta t} \quad (1.2)$$

Taking the limit as $\Delta t \rightarrow 0$, the left side becomes

$$\lim_{\Delta t \rightarrow 0} \frac{m_A(t + \Delta t) - m_A(t)}{\Delta t} = \frac{\partial}{\partial t} (m)_{C.V} = \frac{\partial}{\partial t} \int_{C.V} \rho dV \quad (1.3)$$

Where ρ is the mass density, V indicates volume, and C.V designates the control volume fixed in space and bounded by the control surfaces (S.C).The right side of the equation is

$$\lim_{\Delta t \rightarrow 0} \left\{ \frac{m_A(t + \Delta t)}{\Delta t} - \frac{m_B(t + \Delta t)}{\Delta t} \right\} = m_{in} - m_{out} \quad (1.4)$$

Which becomes,

$$m_{in} - m_{out} = - \int \rho V \cos \alpha dA = - \int_{C.S} \rho V \cdot dA \quad (1.5)$$

Where m_{in} and m_{out} represent the mass rate of flow in and out of the control volume and V is the velocity vector. V is the magnitude of the velocity vector and α is the angle between the velocity vector and the outward normal. Then the continuity equation for the control volumes becomes

$$\int_{C.S} \rho \mathbf{V} \cdot d\mathbf{A} = \frac{\partial}{\partial t} \int_{C.V} \rho dV \quad (1.6)$$

Equation (6) is the integral form of the continuity equation and physically says that the net rate of mass flow out of the control surface is equal to the time rate of decrease of mass inside the control volume. Examine equation (6) by first considering some general simplifications, the some specific examples.

Since the control volume is fixed, the right side of (6) is zero for steady flow ($\partial\rho/\partial t = 0$) giving

$$\int_{C.S} \rho \mathbf{V} \cdot d\mathbf{A} = 0 \quad (1.7)$$

For incompressible flow we have

$$\int_{C.S} \mathbf{V} \cdot d\mathbf{A} = 0 \quad (1.8)$$

Considering the steady flow of Figure 1.4, where the fluid enters section 1 and leaves sections 2 and 3, we have

$$\int_{C.S} \rho \mathbf{V} \cdot d\mathbf{A} = 0$$

$$\int_{A2} \rho V \cdot dA + \int_{A3} \rho V \cdot dA + \int_{A1} \rho V \cdot dA = 0$$

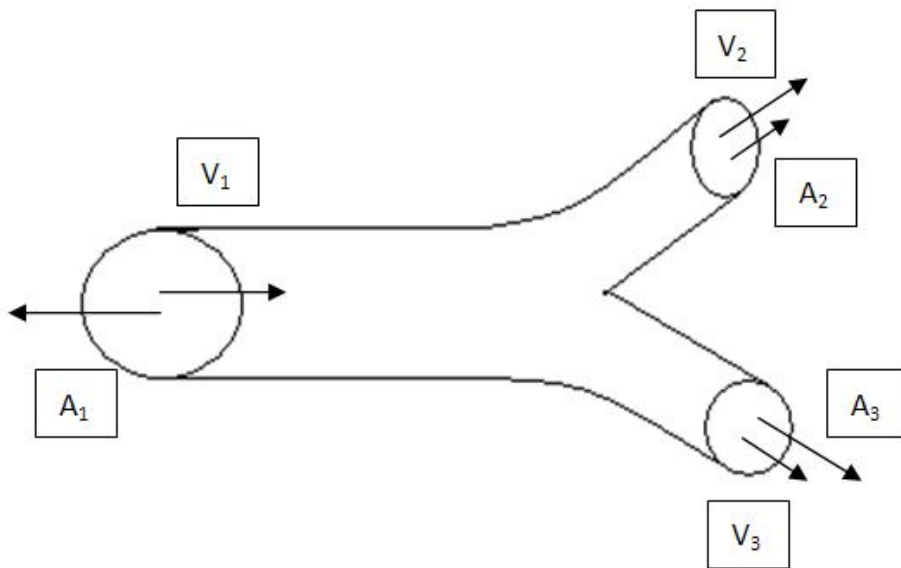


Figure 1.5 Fluid flow in bifurcation design

Assuming that the velocity is normal to all surface where fluid crosses,

$$\int_{A_2} \rho V \cdot dA + \int_{A_3} \rho V \cdot dA - \int_{A_1} \rho V \cdot dA = 0$$

If the densities and velocities are uniform over their respective areas,

$$\rho V_2 A_2 + \rho_3 A_3 V_3 - \rho_1 A_1 V_1 = 0 \quad (1.9)$$

For a single pipe with no third exit the equation becomes

$$\rho V_2 A_2 = \rho_1 A_1 V_1 \quad (1.10)$$

The assumptions made in arriving at equation (1.10) are (a) steady flow, (b) velocities normal to the surfaces, (c) velocity and density constant over the respective areas, and the (d) one exit and one inlet to the control volume.

1.8 OBJECTIVES

The objectives of this project are:

- Investigate effect of bifurcation on blood flow distribution
- Predict flow abnormalities due to blood properties

1.9 SCOPE

The scopes are:

- To analyze flow on bifurcation_based upon different blood properties
- Non Pulsatile blood flow will be used
- Solutions will be based on numerical approach only

CHAPTER 2

LITERATURE REVIEW

2.1 FLOW BEHAVIOR IN MICROVESSEL BIFURCATIONS

Unsteady flow phenomena dominated in blood flow in the arteries. The cardiovascular system is an internal flow loop with multiple branches in which a complex liquid circulates. A nondimensional frequency parameter, the Womersley number, governs the relationship between the unsteady and viscous forces. Normal arterial flow is laminar with secondary flows generated at curves and branches. The arteries are living organs that can adapt to and change with the varying hemodynamic conditions. In certain circumstances, unusual hemodynamic conditions create an abnormal biological response. Velocity profile skewing can create pockets in which the direction of the wall shear stress oscillates.

In recent years, computational techniques have been used increasingly by researchers seeking to understand vascular hemodynamic. Numerous two-dimensional analyses have been performed whereby arteries have been approximated as branched channels. These approximations, although constituting a necessary first step in the development of the computational framework, are largely inapplicable to arterial flow and will not be considered further. In contrast to the large number of two-dimensional solutions, few solutions to the three-dimensional, transient, flow equations governing blood flow have been performed. Of particular interest are the work of Perktold et al. (K.Perktold, 1991) and

the work of Ethier et al. (D.A.Steinman, 1995) who are investigating pulsatile flow in three-dimensional models of bifurcations and bypass grafts.

Software and hardware technologies are emerging which will enable investigators to create idealized and patient-specific vascular models quickly, and to perform analyses combining accurate rheological models of blood, and constitutive relations and mass transport properties for blood vessels. Methods enable the immediate extraction of complete field variations of fluid and solid mechanical quantities. Precisely controlled ‘computational experiments’ with immediate data extraction and reduction, are an ideal means to test hypotheses of vascular function and augment information obtained from imaging, morphologic and molecular biologic methods.

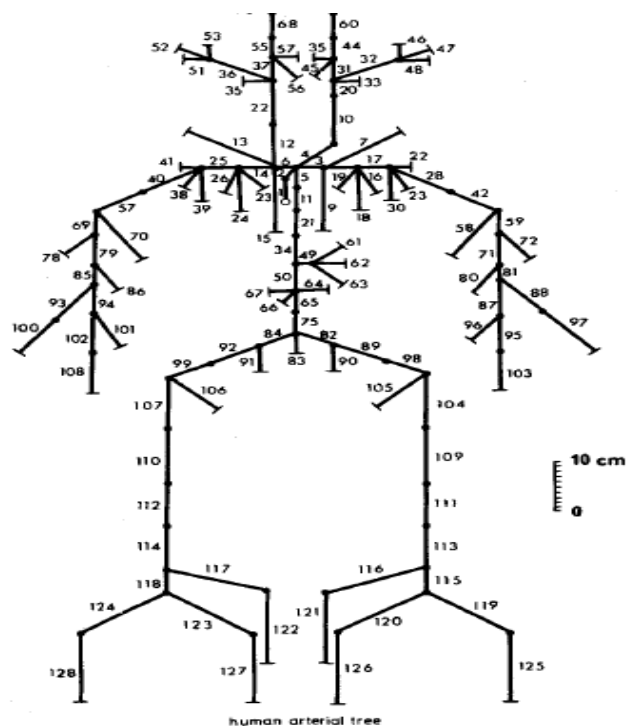


Figure 2.1 Multi branch model of the human arterial system

A.P.Avolio (1980)

2.2 FLOW IN BIFURCATIONS

2.2.1 Coronary arterial flow

As with any other organs in our body, the heart requires blood continuously flowing through its constituent tissue in order to survive. For every minute, the heart pumps out about 5 L of blood. About 5-10% of the output (known as the cardiac output) goes through the coronary vessels. The blood flows through coronary arteries into arterioles and then into capillary beds. It is then channeled through coronary venules and then into coronary veins back into the right atrium. There are, however, certain aspects at which coronary circulation defer from the rest of the circulations in the body. Firstly, the coronary arterial flow occurs during diastole for example during the relaxation phase of the heart cycle while the perfusion of other organs occurs during systole for example during the contraction phase of the cardiac cycle. The other difference is the oxygen extract ratio of the blood flow.

In normal organs, the oxygen saturation of the arterial side is about 96% and on the venous side, the saturation is about 70%. The capillary bed extracts about 25% of the oxygen from the blood that flows through it. Under normal circumstances, however, 70% of oxygen is extracted from the blood flow through coronary capillary bed. The other thing to notice about coronary blood flow is the flows through the coronary vessels are not homogenous. Depending on the heart rate, the flow through sub endothelial (i.e. vessels that are nearest to the ventricular wall) and subepicardial vessels (vessels that are nearest to the pericardial surface) are not the same.

Flows in the heart and great vessels are dominated by inertial forces rather than viscous forces. Reynolds numbers at peak systole are on the order of (Annu. Rev. Fluid Mech. 1997) the flow in the aorta and pulmonary trunk is similar to an entrance type flow that is not developed. Consequently, the core of the flow can be considered an inviscid region that is surrounded by a developing boundary layer at the wall. The pressure and velocity patterns in a complex chamber of the heart can be modeled in three

dimensions, including a moving boundary condition that develops tension (Peskin & McQueen 1989, Yoganathan et al 1994).

Alternatively, in vitro models of the heart and great vessel anatomy can be studied in the laboratory. Flow can now be measured directly in the human heart using techniques such as catheters, Doppler ultrasound, and magnetic resonance velocimetry. These studies show that a large secondary flow in the ventricle is produced by inflow from the atrium through the mitral valve. The secondary flow can persist throughout diastole until the ejection phase. Systolic ejection is similar to a bellows-type flow with lateral pressure creating axial flow out of the aortic valve. In the ascending arch, potential flow theory predicts a skewing of the velocity profile toward the inner wall of the bend. Pressure differences caused by the velocity distributions can account for valve motion and closure (Fung 1984). The abdominal aorta is the large vessel from the heart that traverses the middle of the abdomen and bifurcates into two arteries supplying the legs with blood.

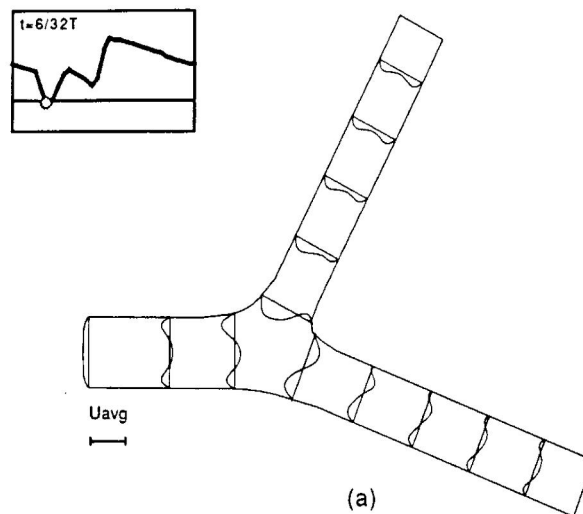


Figure 2.2 The profiles during systole show no flow reversal at the flow divider.

(Journal Biomechanical Engineering, 2001)

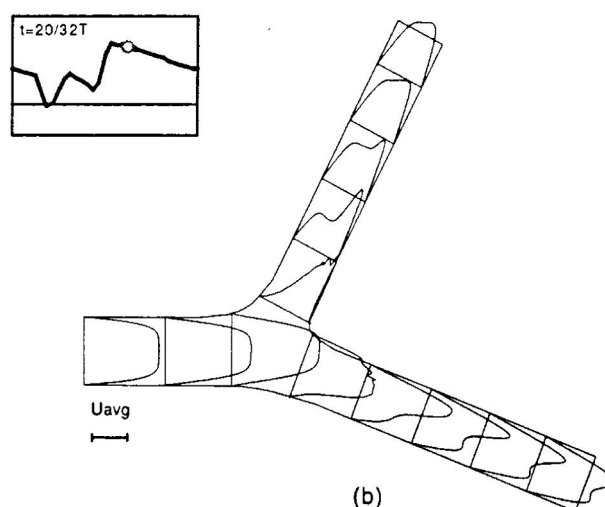


Figure 2.3 The velocity profile during diastole

(Journal Biomechanical Engineering, 2001)

On the upstream end, flow comes from a relatively straight descending thoracic aorta and immediately branches laterally into two renal arteries and anteriorly into the celiac trunk at the level of the diaphragm. The renal arteries have a low resistance so that two thirds of the entering flow leaves the abdominal aorta through these three branches at the diaphragm. During rest conditions, the leg muscle requires little blood flow and has a high resistance. Only one third of the thoracic aorta flow passes into the legs through the abdominal aorta.

Curiously, atherosclerotic disease extends along the posterior wall of the relatively straight abdominal aorta downstream of the renal arteries in all people. Little disease is present in the upstream thoracic aorta. A typical Reynolds number for the abdominal aorta is 600 at rest, but it may increase 10 fold with exercise conditions. The Womersley parameter is about 16 and the lumbar curvatures have an approximate Dean number of 260. Thus one would expect a rather blunt set of velocity profiles and limited amount of velocity skewing (Charles A. Taylor et al.1998).

2.2.2 Cerebral arterial flow

The middle cerebral artery (MCA) carries about 80% of the flow volume received by the cerebral hemisphere. The normal MCA blood velocity (V_{MCA}) under resting conditions ranges from 35 to 90 cm/sec, with a mean of about 60 cm/sec. This range probably reflects the well-known individual MCA diameter variation as well as individual differences in cerebral blood flow. In healthy individuals, V_{MCA} shows CO₂ reactivity of $3.4 \pm 0.8\%$ /mm Hg, which is very close to the $4.1 \pm 1\%$ CO₂ reactivity of cerebral blood flow determined by means of the xenon washout technique. Together, these data suggest the attractive possibility that investigating variations in V_{MCA} may provide a good impression of variations in MCA flow volume (Q_{MCA}) - The present study was conducted to examine in further detail the relation between concomitant variations in V_{MCA} and Q_{MCA} in clinical situations. A special emphasis was placed on evaluating blood velocity measurements as a clinical tool in labile vascular situations since flow measurements using the well-established xenon washout techniques have definite limitations under such circumstances.

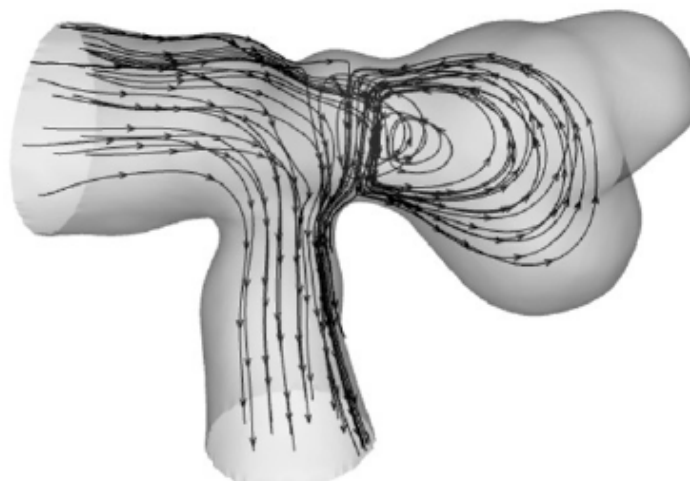


Figure 2.4 Streamlines indicating the complex flow inside the cerebral aneurysm

(J.Bernsdof et al, 2008)

2.2.3 Carotid bifurcation

The flow in a carotid bifurcation model was studied by numerous authors (Bharadvaj et al., 1982a, b; Perktold and Hilbert, 1986; Rindt et al., 1990; Rindt and van Steenhoven 1996; Palmen et al., 1997). In these studies, there are many other investigations on flow in the corresponding author. Large arteries, blood were modeled as a Newtonian fluid. The viscoelasticity of blood was ignored, and using the argument that shear rates in large arteries are predominantly high, the viscosity of blood was taken equal to the high shear rate limit viscosity of blood (3.2 Pa s). Whether or not the assumption that blood can be modeled as a Newtonian fluid is admissible is under dispute. Several numerical studies indicate that the influence of shear thinning properties of blood is not significant for the flow in large arteries (Perktold et al., 1991; Cho and Kensey, 1991). Other studies do and significant influence (Rodkiewicz et al., 1990), or apply scaling procedures while comparing Newtonian and shear thinning fluid models (Baaijens et al., 1993; Ballyk et al., 1994). None of the above studies incorporated the viscoelastic behavior of blood. Experimental studies on non-Newtonian flow in large arteries are relatively sparse, but the ones available indicate a significant influence of the viscoelasticity of the blood analog fluids on the flow phenomena (Liepsch and Moravec, 1984; Ku and Liepsch, 1986).

The flow at the carotid artery bifurcation may have significant bearing on the development and management of atherosclerosis in this major blood vessel. For over a century, hypotheses have linked flow disturbances at this and other arterial branches with the formation of atheromas. Furthermore, advances in noninvasive ultrasound studies of blood velocity in the carotid arteries have pointed to the need for a more rigorous understanding of normal physiologic flow patterns at this branch. Fluid flow patterns at branches are highly dependent on geometry, Reynolds number, and flow division ratios. In the case of human physiology, the flow is additionally pulsatile, introducing a time-dependent behavior. Second order effects which influence the flow, but to a much lesser degree, are the compliance of the arterial wall and the non-Newtonian viscosity of blood.

Recent investigators have described an average geometry of the human carotid bifurcation based on bipanar angiograms and cadaver specimens. Steady flows at physiological Reynolds numbers and flow division ratios have been visualized and quantified. These results indicated circumferential secondary helices in the internal carotid branch, very low wall shear stresses at the outer wall of the sinus, and relatively large shear stresses at the apex and distal end of the sinus as the flow enters the internal carotid artery. No turbulence was observed in those studies. The secondary flow appeared to be influenced most strongly by a flow division between the daughter branches and, to a lesser degree, by the upstream Reynolds number.

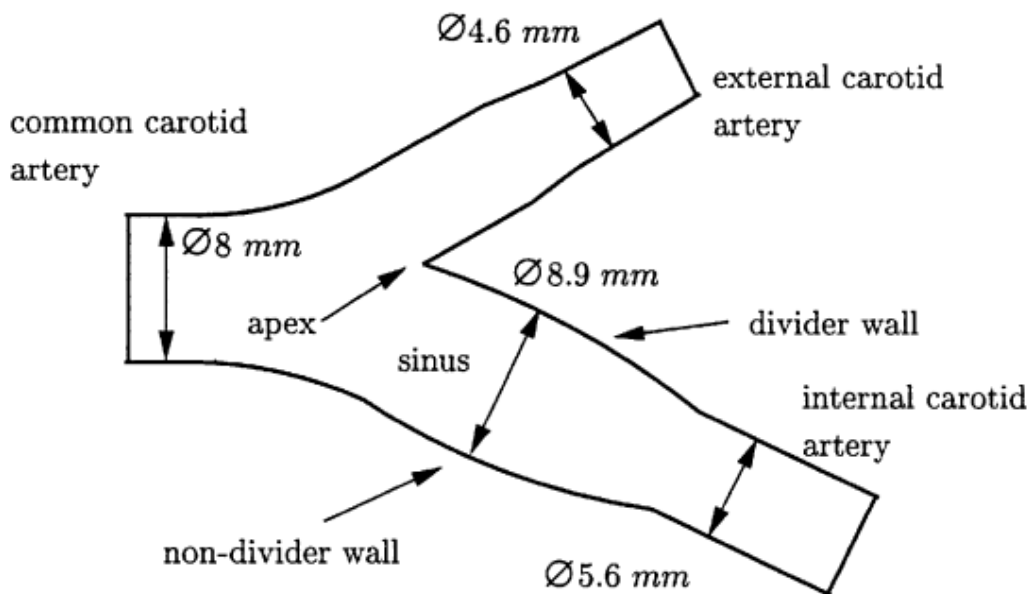


Figure 2.5 Dimension of carotid bifurcation

(F.J.H. Gijsen et al. 1999)

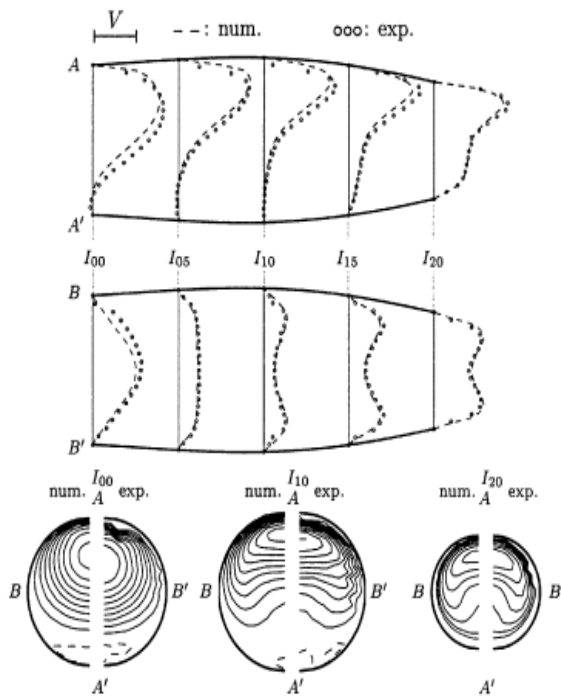


Figure 2.6 Effect on Newtonian fluid

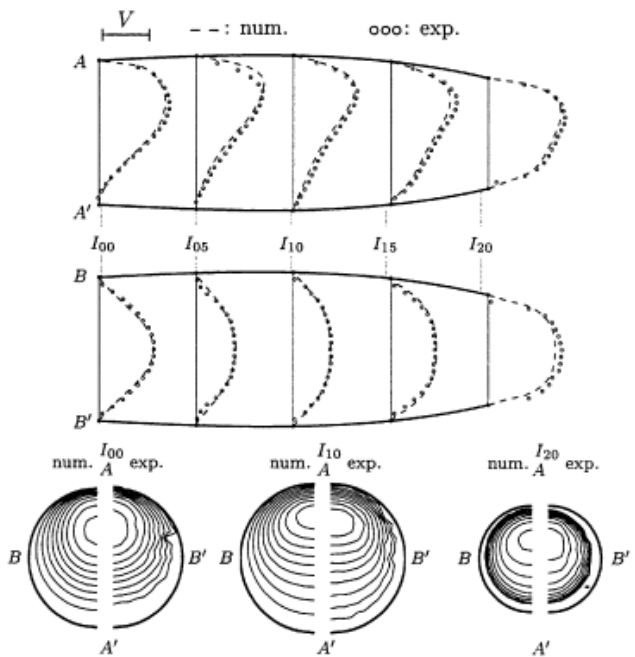


Figure 2.7 Effect on non-Newtonian fluid

(F.J.H. Gijzen et al. 1999)

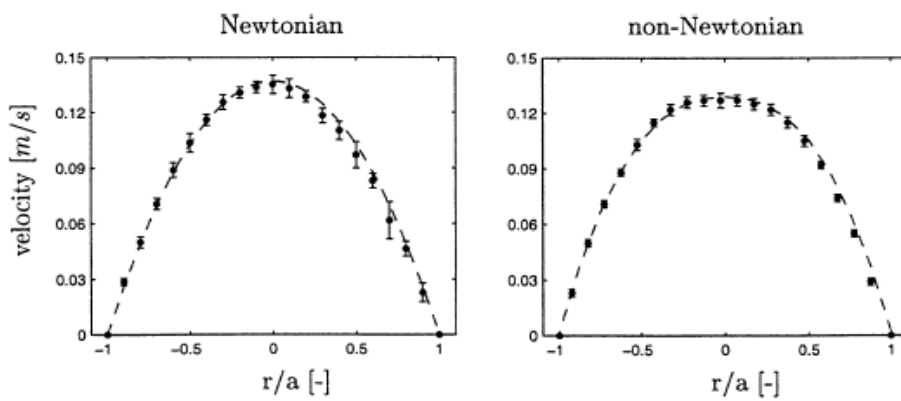


Figure 2.8, Graph for the Newtonian and non Newtonian fluid effect

(F.J.H.Gijzen et.al, 1999)

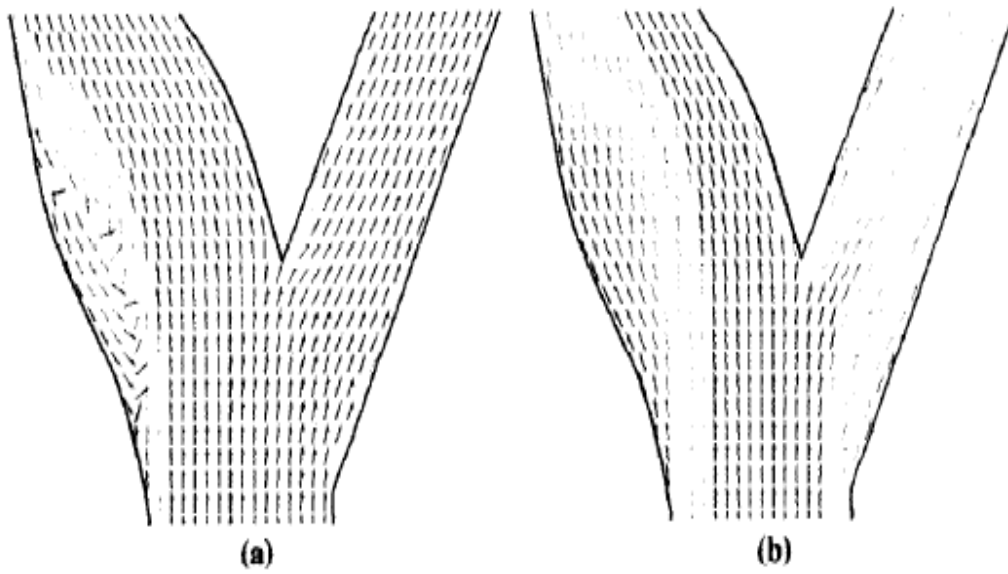


Figure 2.9 Flow for result for pulsatile flow

(CA.Taylor et. Al 1998)

Vortex in carotid flow with Reynolds's Number = 290

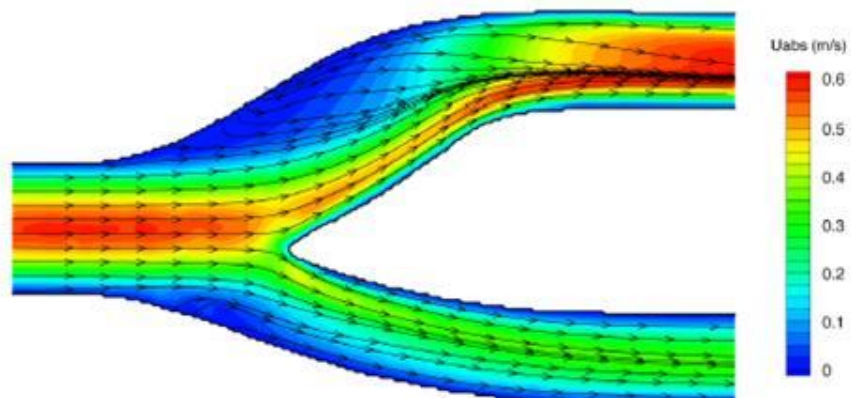


Figure 2.10 Vortex carotid flow using fluent for $Re = 290$

(N. A. Buchmann et al, 2007)

Vortex when increase the value of Reynolds's number = 700

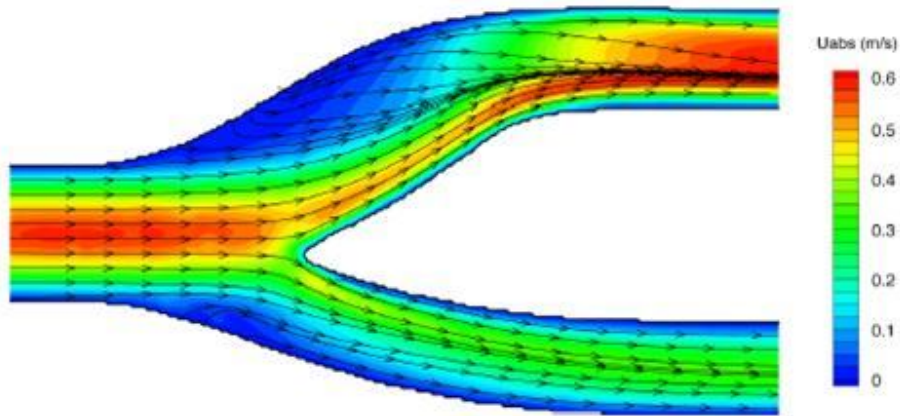


Figure 2.11 Vortex carotid flow for $Re = 700$

(N. A. Buchmann et al, 2007)

2.3 CONCEPT AND THEORY OF BIFURCATIONS

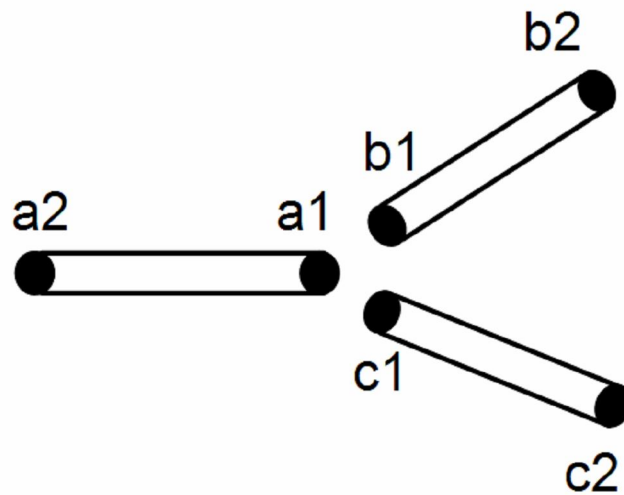


Figure 2.12 Structures of bifurcations

Following the analysis of (Smith et al, 2001) a bifurcation in the arterial network is approximated using three short elastic tubes which are short enough to assume a constant velocity along them and zero losses due to fluid viscosity. No fluid is assumed to be stored within the junction. The grid points associated with each vessel segment are shown in Fig. 2.13,

$$\frac{\partial p}{\partial t} + \frac{1}{2\pi R} \cdot \frac{\partial F}{\partial x} \frac{\partial P}{\partial R} \quad (2.1)$$

Applying the principle of conservation of momentum for tube *a* yields:

$$\pi R_a^2 (p_a - p_o) = \frac{\partial}{\partial t} (\rho l_a \pi R_a^2 V_a) \quad (2.2)$$

Expressions similar to (1) and (12) can be written for tubes *b* and *c*. Expanding these equations using a central difference representation about $(k+1/2)$ time step and further manipulation of the resulting difference equations give:

$$p_{al}^{k+1} - p_{bl}^{k+1} - \frac{2}{\Delta t} (L_a F_a^{k+1}) = -\frac{2}{\Delta t} (L_a F_{al}^k + L_b F_{bl}^k) + p_b^k - p_a^k \quad (2.3)$$

And

$$p_{al}^{k+1} - p_{cl}^{k+1} - \frac{2}{\Delta t} (L_a F_a^{k+1}) = -\frac{2}{\Delta t} (L_a F_{al}^{k+1} + L_c F_{cl}^k) + p_c^k - p_a^k \quad (2.4)$$

Equations (15) and (16) along with conservation of mass given by:

$$F_{al}^{k+1} - F_b^{k+1} - F_c^{k+1} = 0 \quad (2.5)$$

Form a system of three nonlinear equations which are then solved using a Newton-Rhapson iterative scheme which attempts to simultaneously satisfy Equations (2.3) – (2.5).

2.4 CLOSURE

This project will focus on the flow at the branches at the cerebral, aorta and any arteries in the body. The blood parameter will be changes and we will see whether the blood vessel at the branches have a chance to create diseases. In many cases from medical report, the branches are the main part for bloods have a trouble flow and many diseases detect in this area. Arteriosclerosis, aneurysm and high blood pressure are come from the branches. The pressure and the velocity of the blood will be the changes in the analysis using finite volume method in the Computational Fluid Dynamics (CFD). This method is the 1st degree of accuracy method and we cannot use experiment to analysis the data. It is because we do not have a real artery or branches which are difficult to get it. From the analysis with the real condition and parameter, we will conclude that the analysis can get the almost similar result compare to the real one.

CHAPTER 3

METHODOLOGY

3.1 INTRODUCTION

This study is mainly using the Computational Fluid Dynamics (CFD) which consist three parts in the process to get the result. First is pre-processor, then solver and lastly post-processor. All this process is includes in all simulations using CFD to solve problem. Computers are used to perform the millions of calculations required to simulate the interaction of liquids and gases with surfaces defined by boundary conditions. In a mean time, CFD actually using to predict fluid behavior and what would happen in real problem condition.

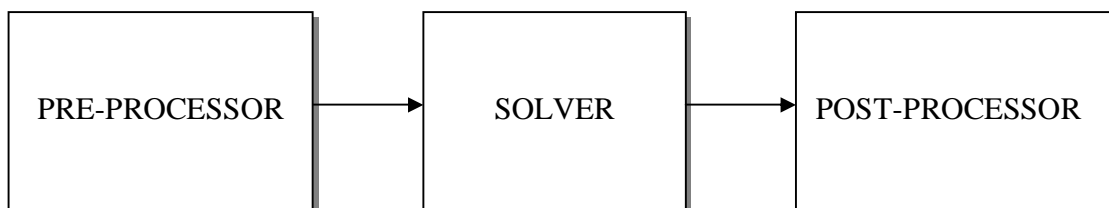


Figure 3.1 Processes in Computational Fluid Dynamics

3.2 SIMULATIONS ASSUMPTION AND PARAMETER

In this study simulations, it is assumed that blood is an incompressible, Non-Newtonian fluid and that the flow is laminar and isothermal a constant viscosity of 0.004 Kg/ (ms). The assumption of non-Newtonian behavior is based on the findings of Perktold et al. (1989) and others who found minimal changes in arterial flow patterns when non-Newtonian effects were included. Furthermore, this assumption is reasonable since the diameter of the internal artery is large enough compared to the size of red blood cell which is about 7.5 μ m. The blood vessel is treated as being rigid because the elastic deformation of the large arteries including cerebral artery is generally less than 10% and the influence is neglected for the main blood flow. The simulation started from the beginning of systole with pressure defined at the artery while the wall was treated as no-slip wall. Then it is repeated to a diastole condition with different pressure. The parameter used in the simulation is listed in Table 3.1.

Table 3.1 Parameter used in simulation

Parameters	Value
Blood pressure	150-463 pa
Blood velocity	0.3-0.7 m/s
Temperature	298 K(constant)
Dynamic Viscosity	0.004 Pa.s
Density	1.12 g/cm ³

3.3 GEOMETRY OF THE MODEL

This study is focus particularly on the model of microvessel bifurcation with different diameter but mainly about 7mm. For the normal and abnormal microvessel bifurcation, the sizes of blood vessel are about 5mm, 7mm, 10mm, 12mm and 14mm. Only for abnormal microvessel, each of them will have an aneurysm with 20mm size.

Modeling was completely done in SOLIDWORK software package with data of the aneurysm parameter taken from literature. The geometries were meshed with the help of the raster approach to investigate the dynamics of blood flow in branches.

These geometries are in good agreement with the real images from the human body. In the simple model the average density and viscosity of whole blood were assumed 1060 kg/m^3 by Cutnell J et al.(1998) and equal to the water viscosity by Pozrikidis C.(2003). The constant inlet pressure of the arteriole was applied as a boundary condition, and by changing the outlet pressure of the arteriole the dynamics of the blood flow was investigated. In addition, because gravity plays only a minor role in the distribution of blood flow by Burrowes KS,(2005), its effect was neglected.

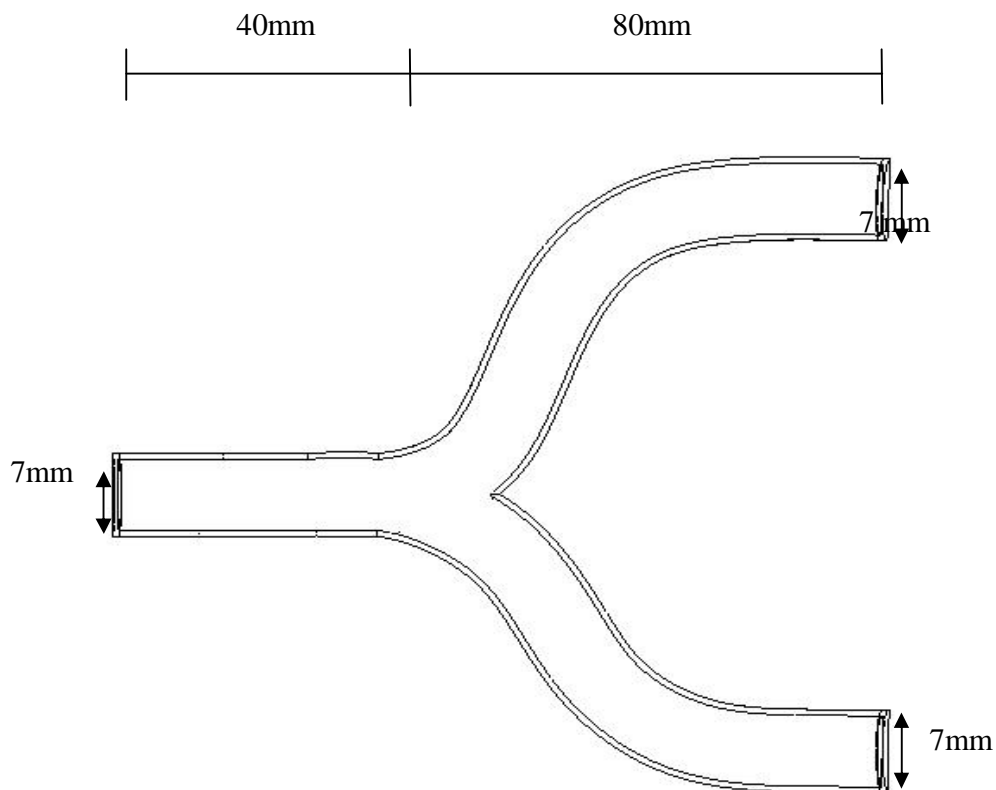


Figure 3.2 Normal microvessel bifurcations models

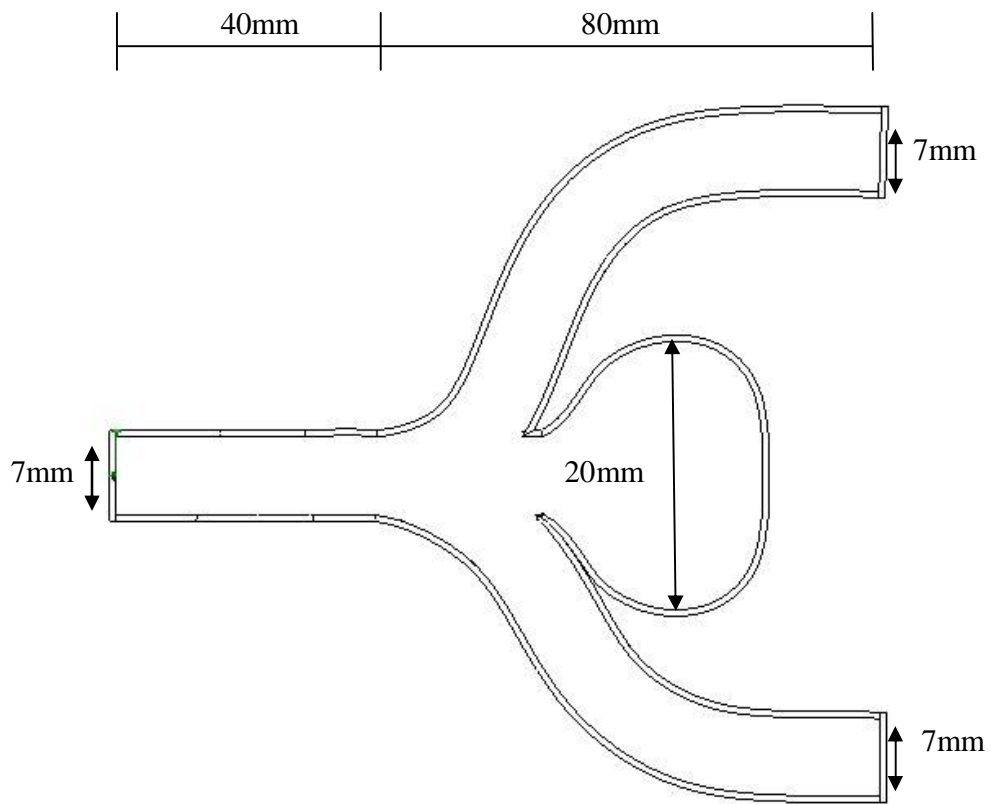


Figure 3.3 Abnormal microvessel bifurcations model

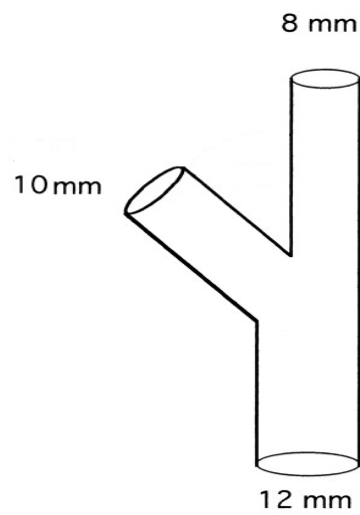


Figure 3.4 The model geometry taken from literature

(Moriyama.Y et al, 1999)

3.4 BOUNDARY CONDITION

After design the geometry of the model, the boundary condition of the analysis was stated. From this study, there are 3 main things in boundary condition to be applied. First is velocity of the blood. The inlet velocity of blood flow when enter to the microvessel is considered 0.3m/s. Actually the velocity would not be constant because blood are pulsatile in the blood vessel depend heart pump rate. Reynold's Number also influence in approaching the blood flow velocity. Second is pressure of blood flow was considered as static pressure. The value is about 463Kpa and blood pressure must be lower than the atmosphere pressure. It is because if the atmosphere pressure higher than human blood pressure, availability of human to be dead is higher. Blood vessel cannot withstand with the difference pressure and it will crack or failed to function. Vascular wall in human body in was created by having elasticity characteristic. In real condition the structure of the vascular wall cannot be real wall that is fixed and not elastic because human body consists of flesh. Only bones have the hard and non elastic wall. That's why the bulge of aorta occurs because the elasticity condition of vascular wall. Maybe the elasticity percentage and factor in the vascular wall of aneurysm region was decrease. In the simulation method, it was oppose with the real condition. We considered the boundary condition to be real wall or rigid because the consideration of elastic wall in this simulation was not possible. Real wall mean the wall not have the elastic properties or rigid.

3.4.1 Initial velocity

From the research by the researcher from United States, he has done the analysis about blood velocity and he concludes that the velocity profile in averages is 0.2-0.4 m/s. (Jorgen.A.J, 1993).

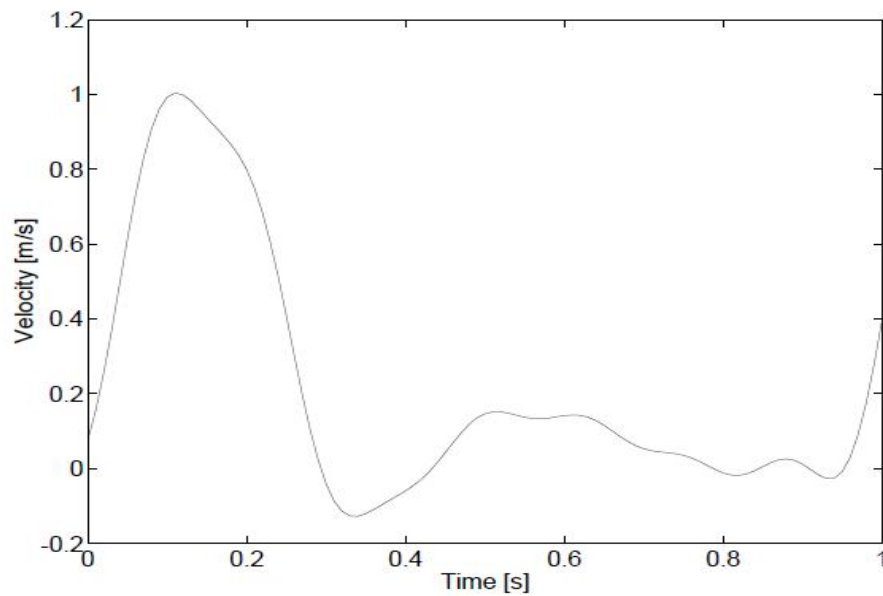


Figure 3.5 Graph of the blood velocity profile in common femoral artery.

(Jorgen.A.J, 1993)

From Jorgen.A.J researched in 1993, the result on velocity profile was in common femoral artery. The velocity is lower than the inlet velocity for this study analysis is because femoral artery is far from heart. This result can be considered as one of the proved the velocity blood flow will be lower when far from the heart.

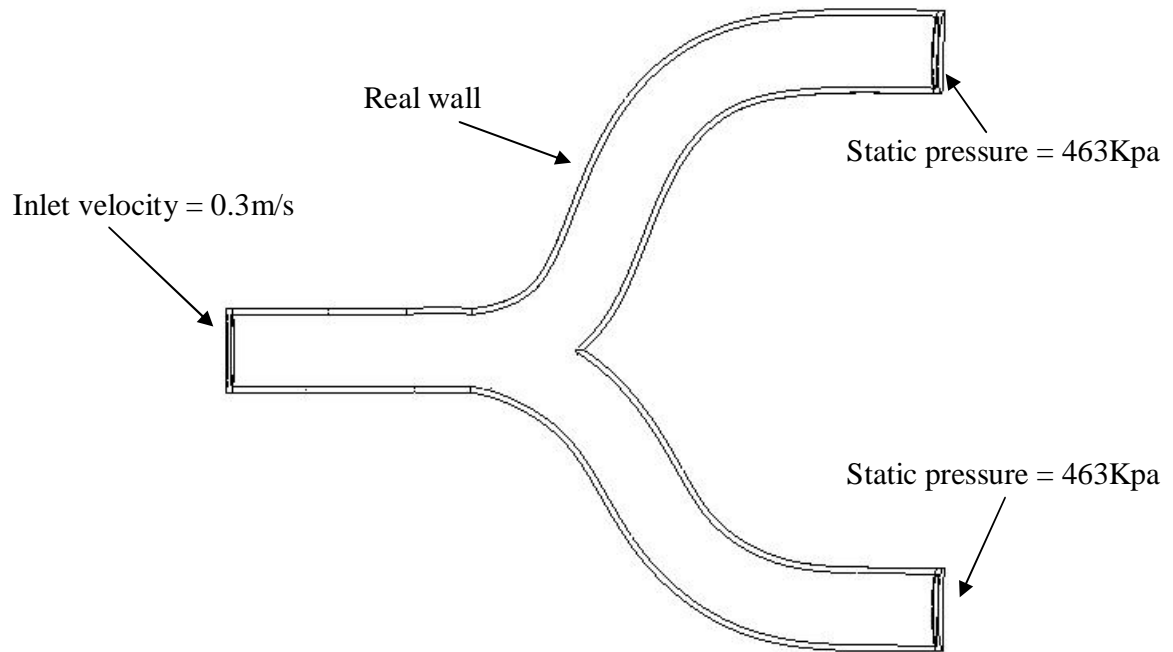


Figure 3.6 Pressure input for normal blood vessel model

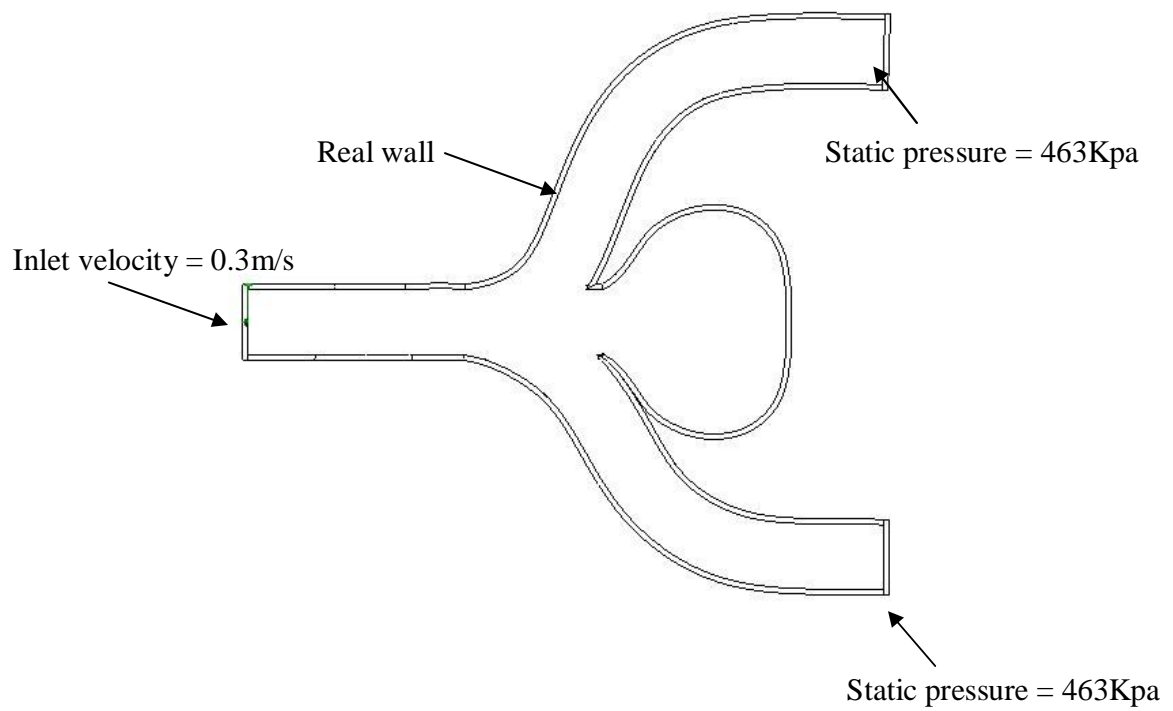


Figure 3.7 Pressure input for abnormal blood vessel

3.5 GOVERNING EQUATION OF BLOOD FLOW

Blood flow in artery is considered to be incompressible, consisting of the continuity and Navier-Stokes equations. The governing equations are written as follows for a computational domain Ω :

$$\frac{\partial u_i}{\partial x_i} = 0 \quad (1)$$

$$\rho \left(\frac{\partial u_i}{\partial t} + u_j \frac{\partial u_i}{\partial x_j} \right) = -\frac{\partial P}{\partial x_j} + \mu \frac{\partial^2 u_i}{\partial x_j \partial x_j} + f_i \quad (2)$$

u_i = velocity in the i^{th} direction

P = Pressure

f_i =Body force

ρ =Density

μ_i =Viscosity

δ_{ij} =Kronecker delta

The shear stress, τ at the wall of aneurysm calculated base on a function of velocity gradient only:

$$\tau = \mu \frac{\partial u}{\partial y} \quad (3)$$

Where $\partial u/\partial y$ is the velocity gradient along the aneurismal wall taking considerations of fluid viscosity. Therefore, the simple viscous fluids considered with linear relationship. The equation of motion in terms of vorticity, ω as follows:

$$\frac{\partial \omega}{\partial t} - \nabla \times (\nabla \times \omega) = \frac{\mu}{\rho} \nabla^2 \omega \quad (4)$$

Where ω is the vorticity, ρ =Density and μ = viscosity with vector $\nabla^2 V$ evaluated a well. Solution of these equations in their finite volume form is accomplished through a commercial software package, CAE-CFD. The Navier-Stokes equations for 3D laminar flow with were solved using a finite-volume based CFD solver integrated.

3.6 FINITE VOLUME METHOD

This study only uses numerical approach on doing an analysis. In Computational Fluid Dynamics, finite volume method have used to solve the equation and to stimulate the blood flow. The finite volume method is a method for representing and evaluating partial differential equations in the form of algebraic equations [LeVeque, 2002; Toro, 1999]. Similar to the finite difference method, values are calculated at discrete places on a meshed geometry. Finite volume refers to the small volume surrounding each node point on a mesh. In the finite volume method, volume integrals in a partial differential equation that contain a divergence term are converted to surface integrals, using the divergence theorem. These terms are then evaluated as fluxes at the surfaces of each finite volume. Because the flux entering a given volume is identical to that leaving the adjacent volume, these methods are conservative. Another advantage of the finite volume method is that it is easily formulated to allow for unstructured meshes. The method is used in many computational fluid dynamics packages call COSMOSFloWorks.

FVM is the ideal method for computing discontinuous solutions arising in compressible flows. Any discontinuity must satisfy the Rankine-Hugoniot jump condition which is a consequence of conservation. Since finite volume methods are conservative they automatically satisfy the jump conditions and hence give physically correct weak solutions. FVM is also preferred while solving partial differential equations containing discontinuous coefficients.

3.7 VISUALIZATION OF SIMULATIONS

Last step in the simulation is to show the result of simulation. This step was called post-processor. The only way to analyze blood flow behavior is by this step. In this step, the data calculated by the computer will be interpreted into visual or readable images. The important aspect to visualize the result of the simulation was to analyze, discuss and conclude the simulation that had been done. Furthermore, the result shown was important to validate the result with the previous literature review whether it have similarity or not. Post processor not only consists of flow streamlines, it was also consisting of graph, flow trajectories, animation and others. Figure 3.8 below show the result of the simulation in normal microvessel model of this project.

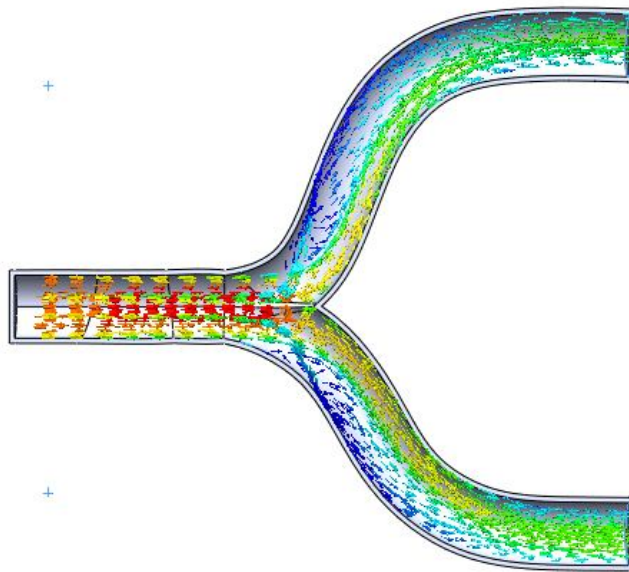


Figure 3.8 Visualization of blood flow streamlines in normal microvessel

CHAPTER 4

RESULT AND DISCUSSION

4.1 RESULT

Computational fluid dynamic simulations using the finite volume method have been applied to assess local changes of velocity and diameter in size of blood vessel, and these hemodynamic parameters are fairly well understood. The impact of changes the velocity and the diameter give a different flow patterns behavior at the microvessel bifurcations. With the constant of a few parameters in the analysis such as the density of the blood, ρ and also the dynamics viscosity of blood, μ , and the analysis will be easier to determine. In this study, the effect of microvessel bifurcation has been proven in changes the velocity of the blood flow and increasing the size diameter of blood vessel. The data analysis was compared for different types of microvessel bifurcation analysis establish the correlation velocity, pressure and blood flow behavior.

The discussion on Reynold's Number also includes in this analysis. Using the assumption the blood flow is laminar, the analysis on Reynold's Number can proved the assumption was correct. These discussion on the velocity of blood flow and change of diameter blood vessel can be effect by the bifurcation were to validate the results with previous numerical simulation by other researcher. The other parameters obtained are reliable because the initial validation results on velocity agreed with the current numerical simulation.

4.2 VELOCITY BLOOD FLOW

Velocity in the blood flow shown in figure 4.1 interaction between the blood flow and the aneurysm wall. When the velocity of the blood flow has an increment 0.1m/s, the flow pattern are different. The highest velocity is 0.759m/s in the normal blood vessel with the inlet velocity, $v_{inlet} = 0.7\text{m/s}$ in the 7mm diameter of blood vessel. The lowest velocity is 0.136m/s which the values came from the inlet velocity, $v_{inlet} = 0.3\text{m/s}$ with the same diameter of blood vessel. The highest velocity in the abnormal blood vessel which have aneurysm at the arterial is 0.7715m/s with the inlet velocity, $v_{inlet} = 0.7\text{m/s}$. For the lowest values is 0 m/s for almost case in the abnormal blood vessel analysis. This happen because lack of blood velocity which going through the aneurysm. This mean, the aneurysm make an effect in the velocity of blood in the blood vessel and this will increase of pressure in the blood vessel.

From both figure 4.1 and 4.2, the velocity of blood flow decreasing after hit the wall at the branch of blood vessel. Then, when the blood touched the wall at branches, the other particles of blood will separately break. The simulation was shown that no more blood particles at the upper wall of blood vessel. The comparison result of velocity is from the research from Jorgen.A.J which gives the blood velocity profile in common femoral artery. The result from the analysis validated with the femoral artery velocity profile. This proved the data analysis was correct.

The velocity of the blood flow will decrease when it going through the aneurysm blood vessel arterial model. From the result, the behavior of blood flow is different with the normal blood vessel compare to the other model which has aneurysm. For the normal microvessel bifurcation, the velocity of blood flow data gives higher values than the abnormal microvessel bifurcation. According the theory of internal fluids, when the velocity increase, the pressure will decrease and vise versa. So, this will prove that data analysis is correct and proved the concept theory of fluids.

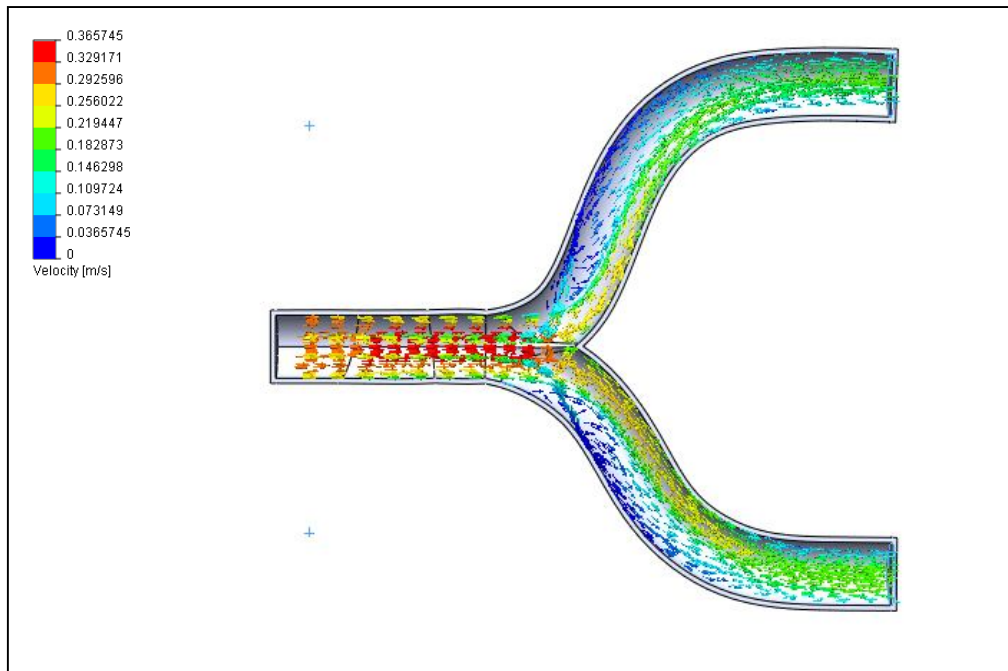


Figure 4.1 Velocity flow for normal microvessel bifurcations

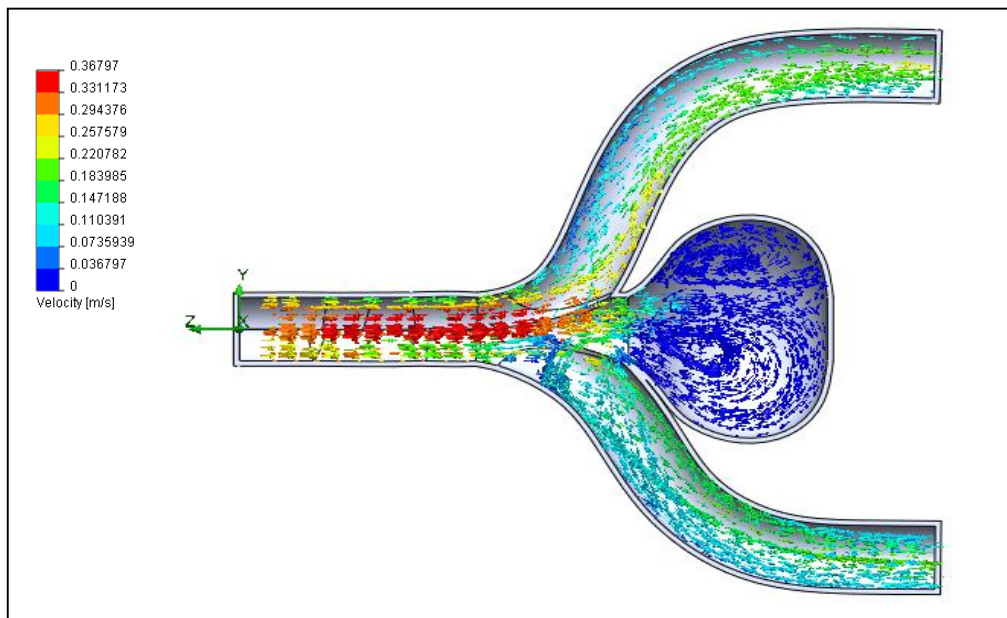


Figure 4.2 Velocity flow for abnormal microvessel bifurcations

Figure 4.3 and 4.4 below will show the result for changes of velocity in same diameter of blood vessel which is 7mm. Velocity blood flow changes increase about 0.1m/s for each analysis.

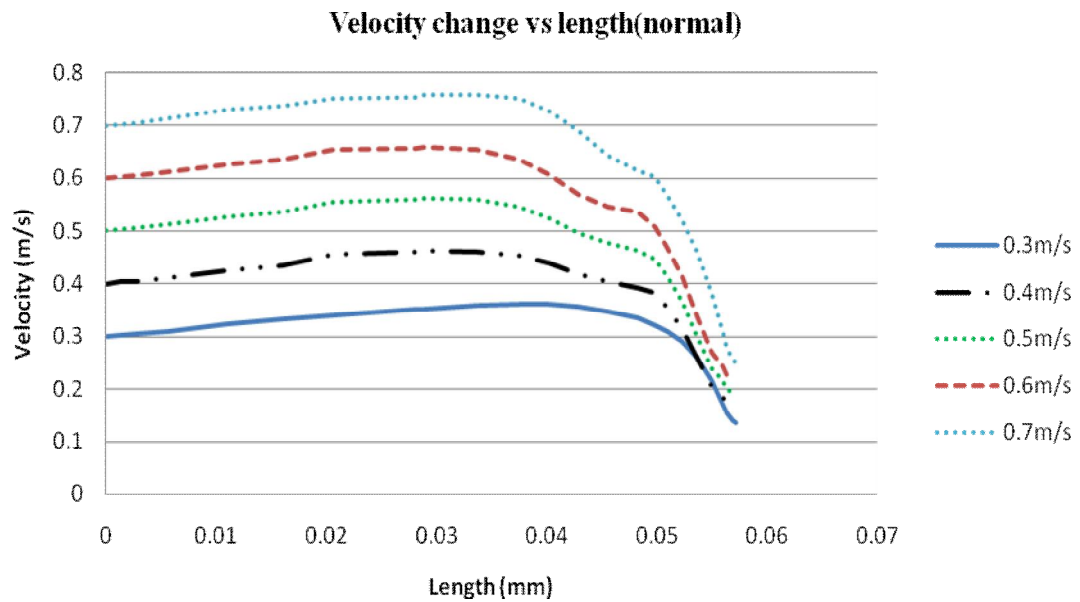


Figure 4.3 Graph velocity vs length for different velocity in normal case

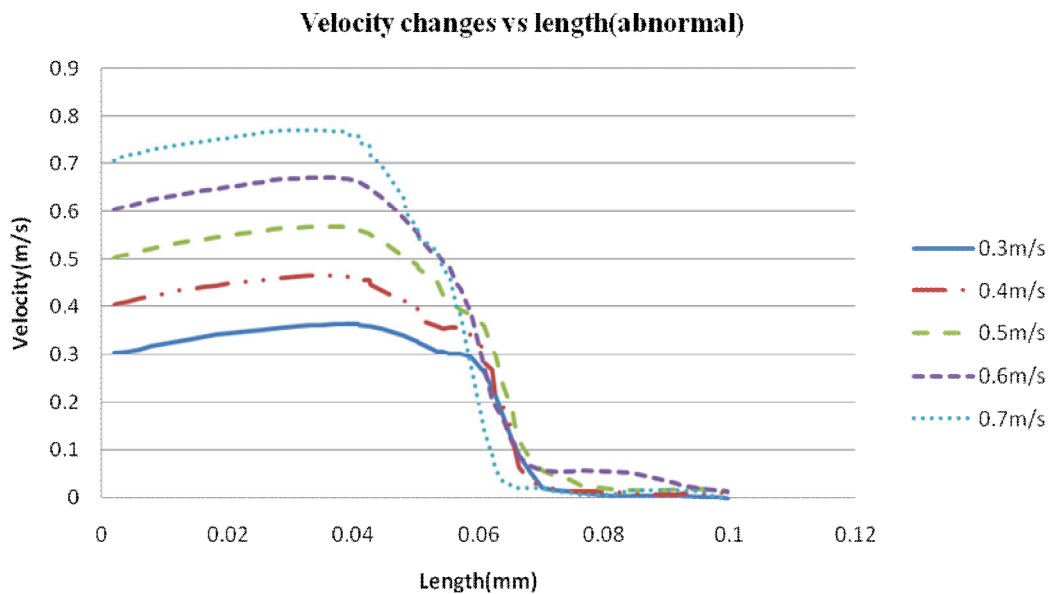


Figure 4.4 Graph velocity vs length for different velocity in abnormal case

In order to explain the result from analysis in different velocity for same diameter, the concept of fluids must be applied. Inlet velocity, V_{inlet} started at 0.3m/s until 0.7m/s have been attached to the entire model in boundary condition for simulation. Then, all the static pressure will be constant which is equal to 463 Kpa. The increment of velocity was about 0.1m/s and the result show from the figure 4.3 and 4.4. For normal microvessel, the velocity smoothly decrease and have slightly effected by the bifurcation. There was a few different for abnormal case. The velocity had decreased mostly at 0.06 to 0.08 meter. Aneurysm at the bifurcation gives a large impact to the velocity blood flow. The velocity blood flow became zero at the end.

Figure 4.5 and 4.6 below shown about the result analysis for normal and abnormal microvessel but with the constant velocity. This time the diameter of blood vessel will be changes and the effect shown in the graph.

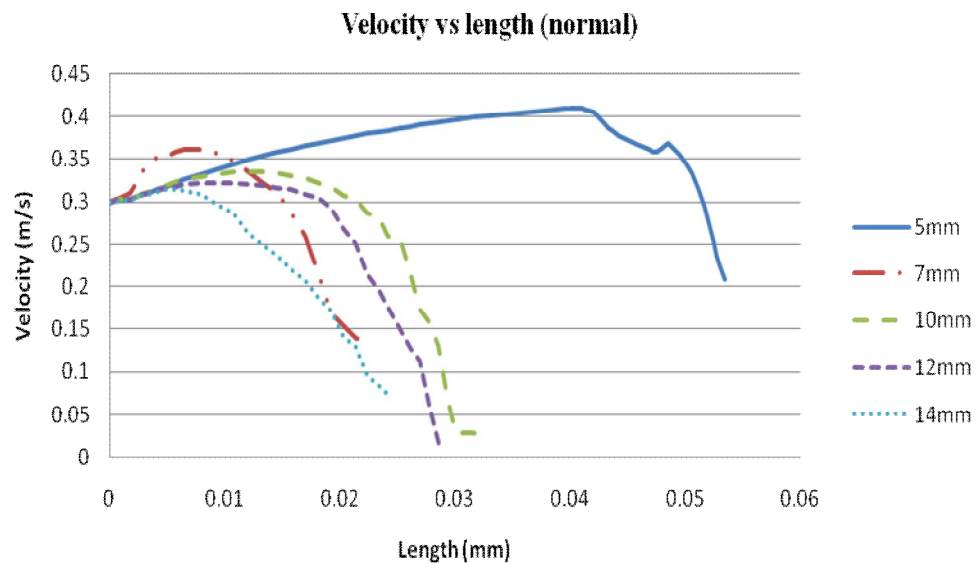


Figure 4.5 Graph velocity vs length for different diameter in normal case

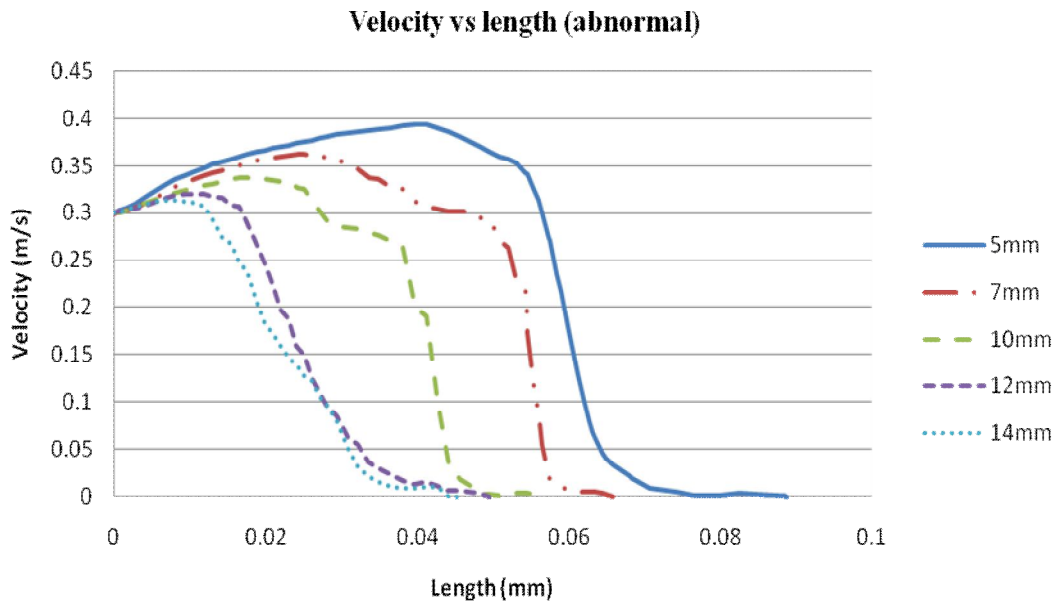


Figure 4.6 Graph velocity vs length for different diameter in abnormal case

In the figures above, the result has shown two cases which are velocity for different diameter in normal and abnormal case. The cases above had shown the effect of diameter in making the velocity of blood going more smoothly when it becomes bigger in size of diameter. These analysis also noted that the bifurcation give an effect to the result of blood parameter. For normal case, the velocity blood flow when the diameter 5mm is higher than bigger diameter of blood vessel. It also happens for abnormal microvessel case. This means the velocity of blood going smoothly through the small diameter of blood vessel rather than the bigger size of diameter. Diameter of blood vessel gives an influence to the blood flow at the bifurcation.

All the simulation figures shown below are when the diameter of blood vessel has been changes. Blood flow behavior shown a different pattern when the diameter of blood vessel increases.

For normal microvessel bifurcations

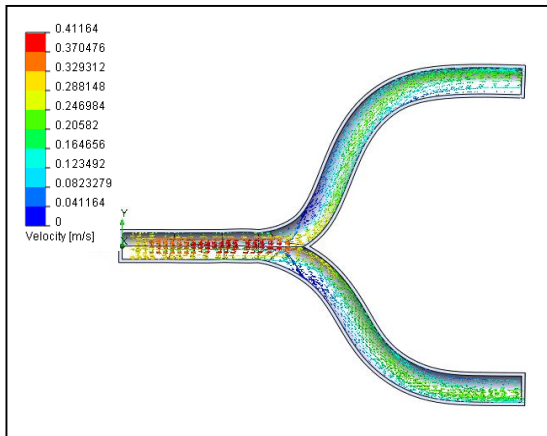


Figure 4.7 Velocity flow for diameter 5mm

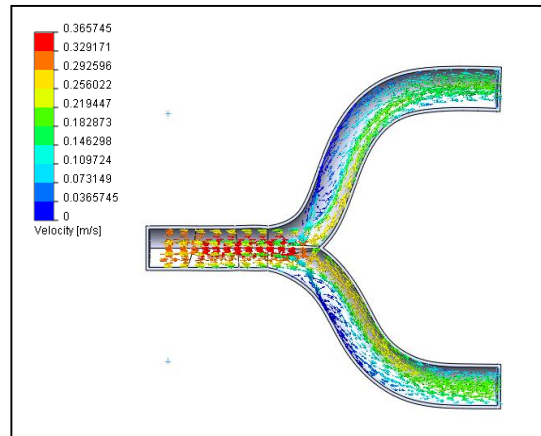


Figure 4.8 Velocity flow for diameter 7mm

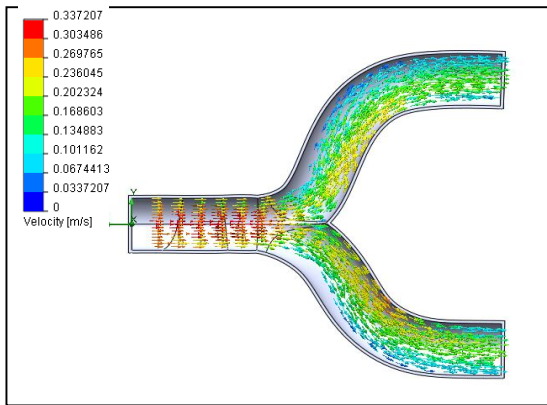


Figure 4.9 Velocity flow for diameters 10mm

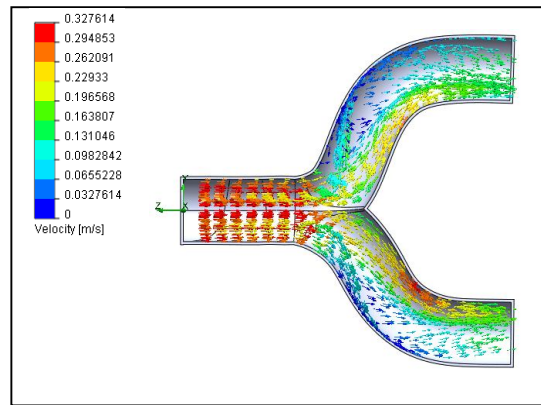


Figure 4.10 Velocity flow for diameter 12mm

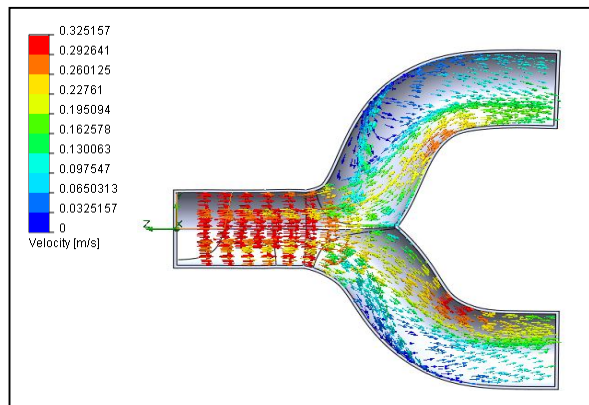


Figure 4.11 Velocity flow for diameter 14mm

For abnormal microvessel bifurcations,

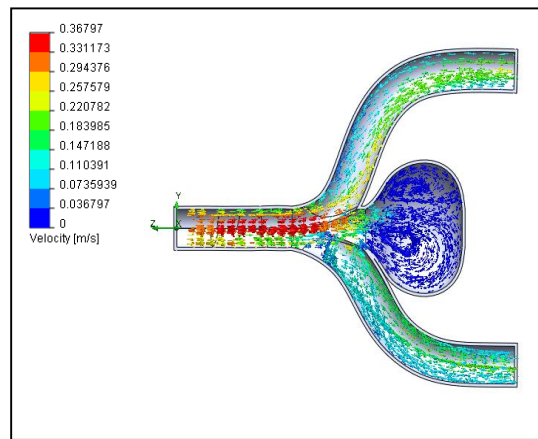
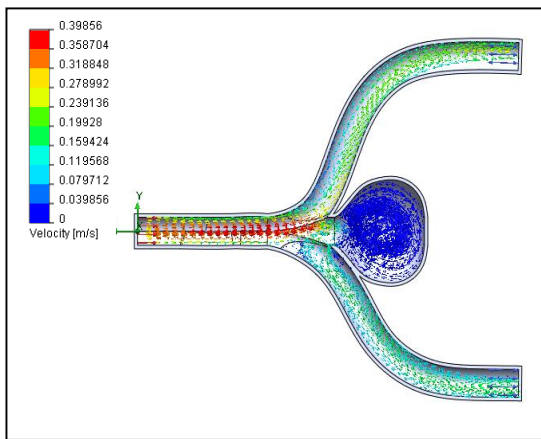


Figure 4.12 Velocity flow for diameter 5mm **Figure 4.13** Velocity flow for diameter 7mm

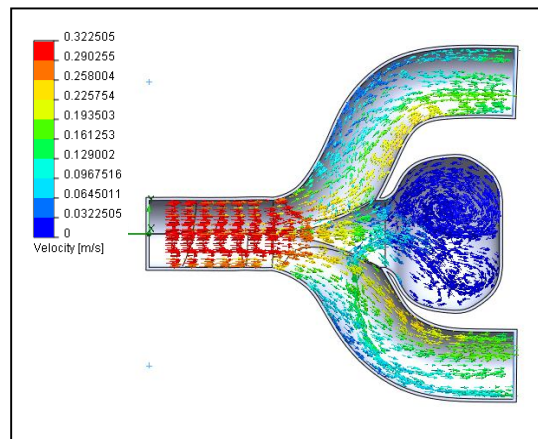
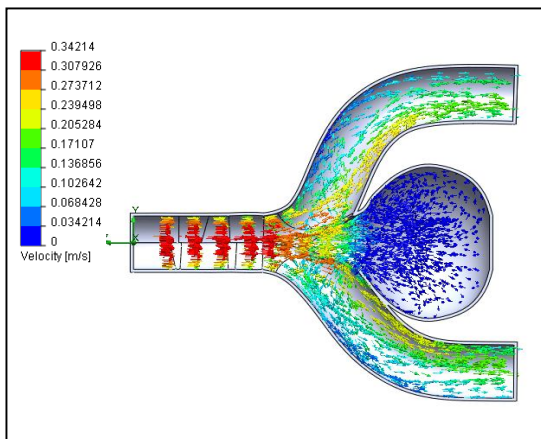


Figure4.14 Velocity flow for diameter 10mm **Figure4.15** Velocity flow for diameter12mm

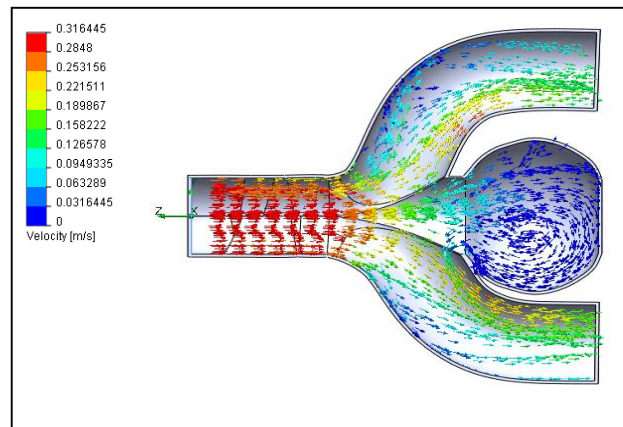


Figure 4.16 Velocity flow for diameter 14mm

Peak velocity also considered in this analysis to know the effect of diameter changes in the microvessel bifurcations. The graph below had shown the different between the normal and abnormal blood vessel on peak velocity vs diameter.

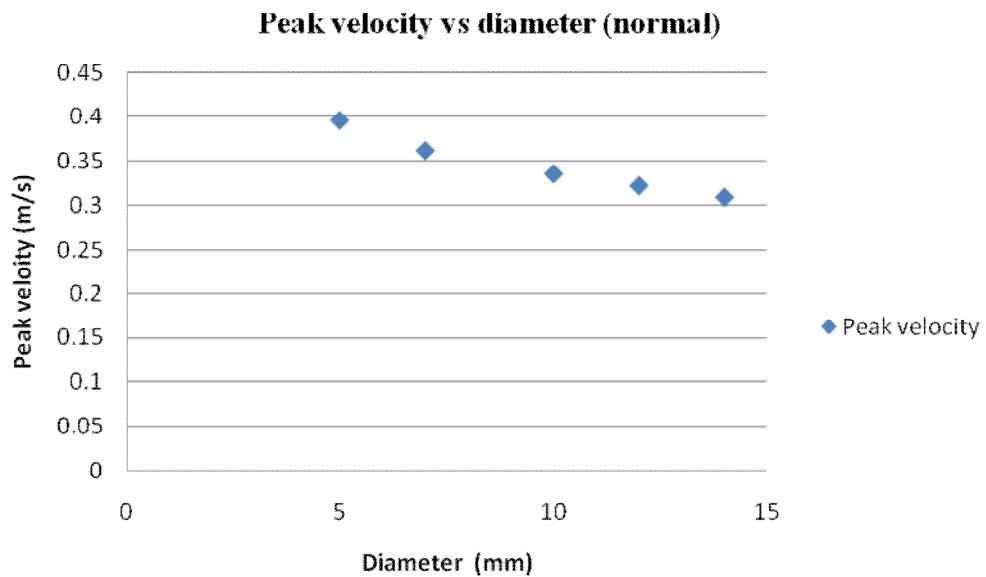


Figure 4.17 Peak velocity vs diameter for normal case

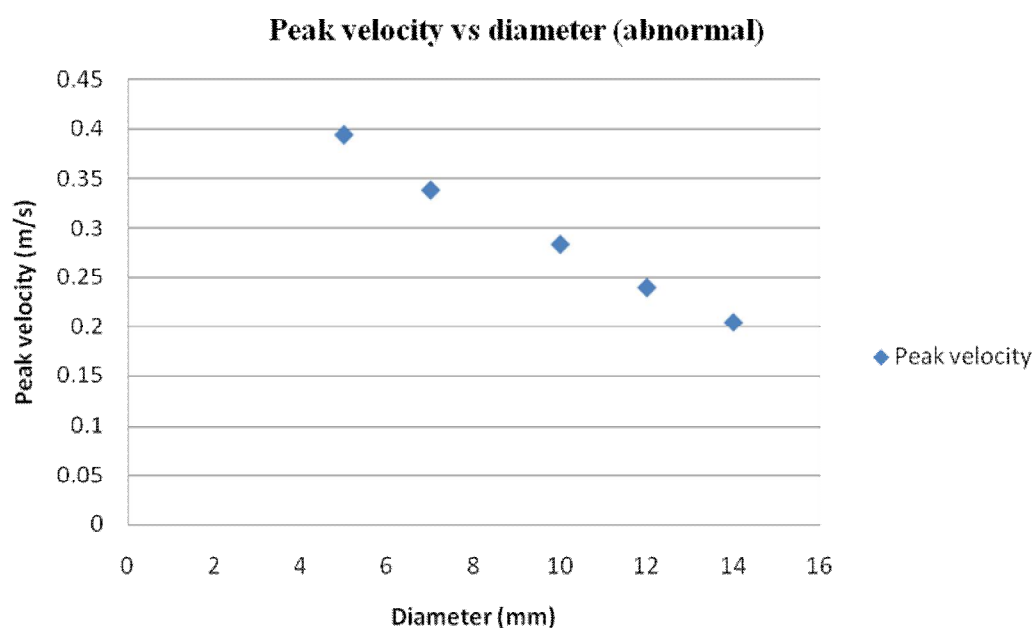


Figure 4.18 Peak velocity vs diameter for abnormal case

From the figure above, the different peak velocity percentage will get a bigger margin when it comes bigger diameter. The different peak velocity percentage for 5mm only about 0.61% and for 7mm it is about 6.4%. The normal case and abnormal case shown the different in peak velocity when the blood going through the aneurysm and without aneurysm. The velocity of the blood will decrease when it comes into the aneurysm. It means, the aneurysm at the branches of the microvessel bifurcations give an effect to the blood flow behaviour

The different percentage for 10mm, 12mm and 14mm diameter of blood vessel also can be proved that the velocity of the blood will decrease after the aneurysm. These will lead to the changes of behaviour of the blood flow and affect the blood vessel. The researcher before done a research on the aneurysm and how to decrease the blood flow turn in the aneurysm. The study will give the reason why the researcher do not want the blood flow into the aneurysm.

Table 4.1 Peak velocity vs diameter

Diameter,mm	Peak velocity, m/s	
	Normal case	Abnormal case
5	0.3961	0.3937
7	0.3617	0.3385
10	0.3352	0.2836
12	0.3220	0.2397
14	0.3091	0.2041

Manual calculation for percentage different for normal and abnormal case,

$$\frac{\text{Normal case} - \text{abnormal case}}{\text{Normal case}} \times 100\%$$

For 5mm,

$$\frac{0.3961 - 0.3937}{0.3961} \times 100\% = 0.61\%$$

For 12mm,

$$\frac{0.3220 - 0.2441}{0.3220} \times 100\% = 21.1\%$$

For 7mm,

$$\frac{0.3617 - 0.3385}{0.3617} \times 100\% = 6.4\%$$

For 14mm,

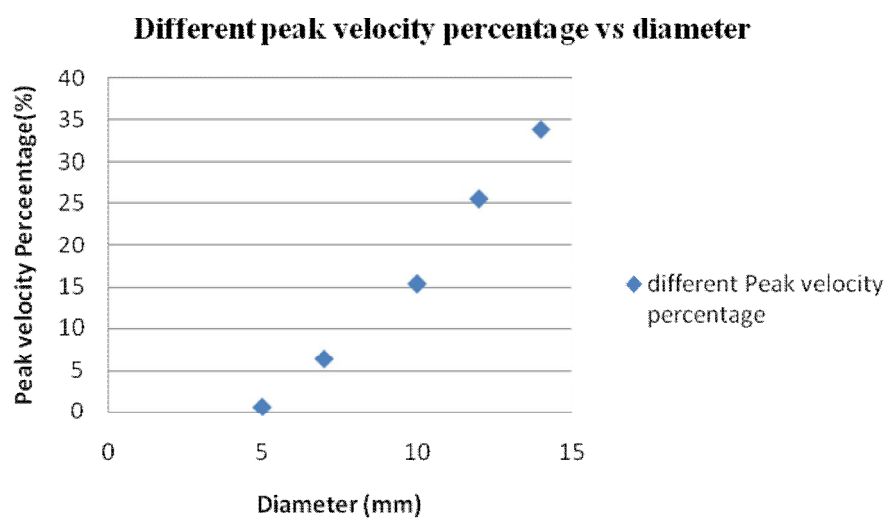
$$\frac{0.3091 - 0.2041}{0.3091} \times 100\% = 33.9\%$$

For 10mm,

$$\frac{0.3352 - 0.2836}{0.3352} \times 100\% = 15.4\%$$

Table 4.2 Peak velocity percentage vs diameter

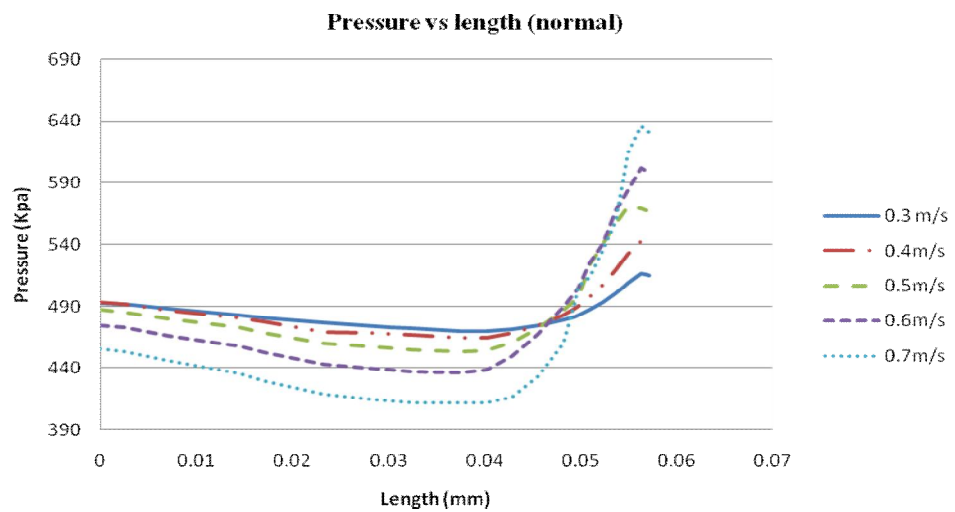
Diameter,mm	Percentage peak velocity different,%
5	0.61
7	6.4
10	15.4
12	21.1
14	33.9

**Figure 4.19** Graph percentage peak velocity different vs diameter

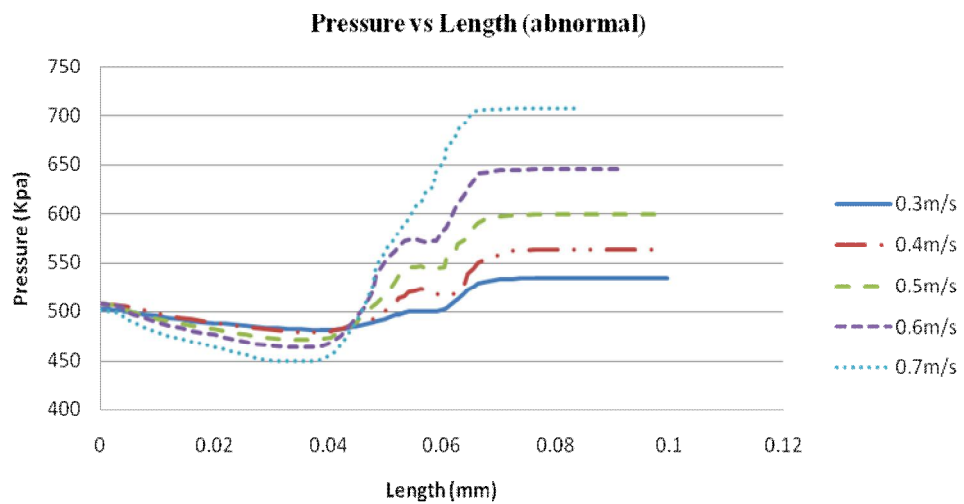
From the graph shown in figure 4.22, normal microvessel and abnormal microvessel have a different peak velocity. When increasing the diameter of the blood vessel, the different of peak pressure also increase. Normal microvessel have higher peak velocity than abnormal microvessel. This mean also, bifurcation make the velocity of blood flow become lower even the microvessel do not have any aneurysm in it. Flow pattern also effected by this phenomena at the bifurcation.

4.3 PRESSURE BLOOD FLOW

The pressure of the blood were also been changed in order to get the different result from a variables of problem. Figure 4.19 and 4.20 had shown the graph analysis for pressure vs length in different velocity in constant 7mm diameter of blood vessel.



4.20 Graph pressure vs length for different velocity in normal case



4.21 Graph pressure vs length for different velocity in abnormal case

From the graph had shown the different of pressure pattern in normal and abnormal microvessel bifurcation. In normal microvessel, the result show that the pressure were slightly increase between length of 0.04-0.06m. The increment of velocity from 0.3m/s to 0.7m/s give a different values of pressure. It is because there are no obstacles like aneurysm at the bifurcations so that the form of blood will just going through the blood vessel. Different with the abnormal microvessel, the blood pressure increase randomly in velocity. When the blood is going through the aneurysm, the pressure increase and it is repeated when the velocity changes in same diameter of microvessel bifurcations. The result means aneurysm give an effect to the pressure of blood at the microvessel bifurcation and give different flow pattern behavior.

Figure 4.21 and 4.22 has shown the graph for changes the diameter of blood vessel. The velocity of blood will be constant in this case.

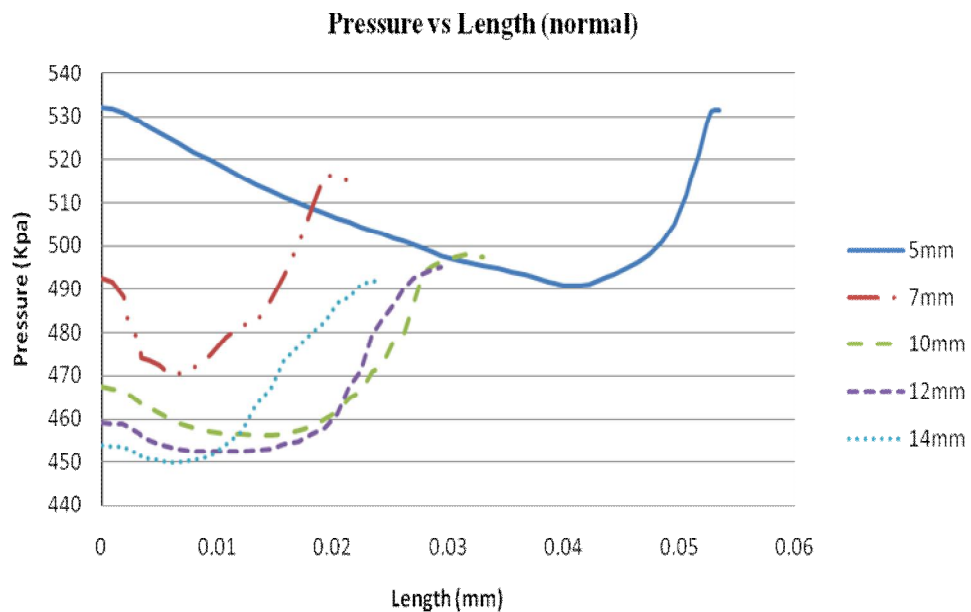


Figure 4.22 Graph pressure vs length for different diameter in normal case

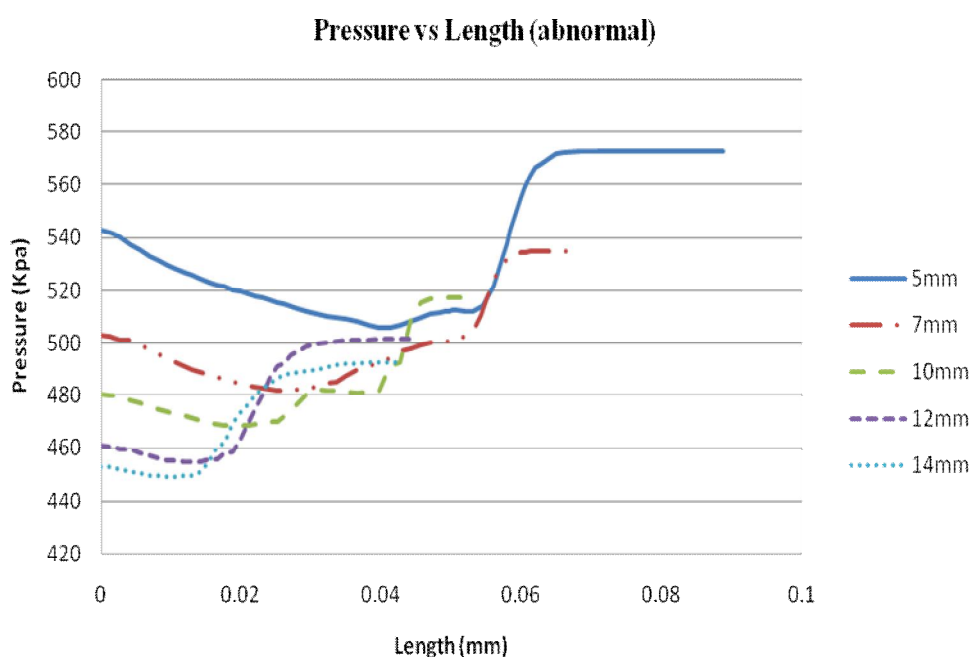


Figure 4.23 Graph pressure vs length for different diameter in abnormal case

These two figures had shown a very different result in pressure vs length. For normal microvessel, the result from analysis had shown that the smaller diameter make a higher pressure than bigger size diameter of blood vessel. It proved that the theory of fluid which is the smaller the open area, the higher the pressure of fluids. The decrement of blood pressure for normal microvessel more smoothly than the abnormal once. The effect of bifurcation can see on these two types of blood vessel and aneurysm give more impact to the blood pressure behavior. For diameter 5mm, normal microvessel has shown the smooth result especially at the length 0.04mm to 0.06mm. At same diameter for abnormal microvessel, the pressure increase slightly at the same length of analysis. Aneurysms at the bifurcation give an impact to the value of blood pressure. It strongly proved that bifurcation and aneurysm give an effect to the blood behavior including velocity and pressure. The blood pressure in this case of study also showed the positive result. It can be a benchmark for other researcher to study more in this case.

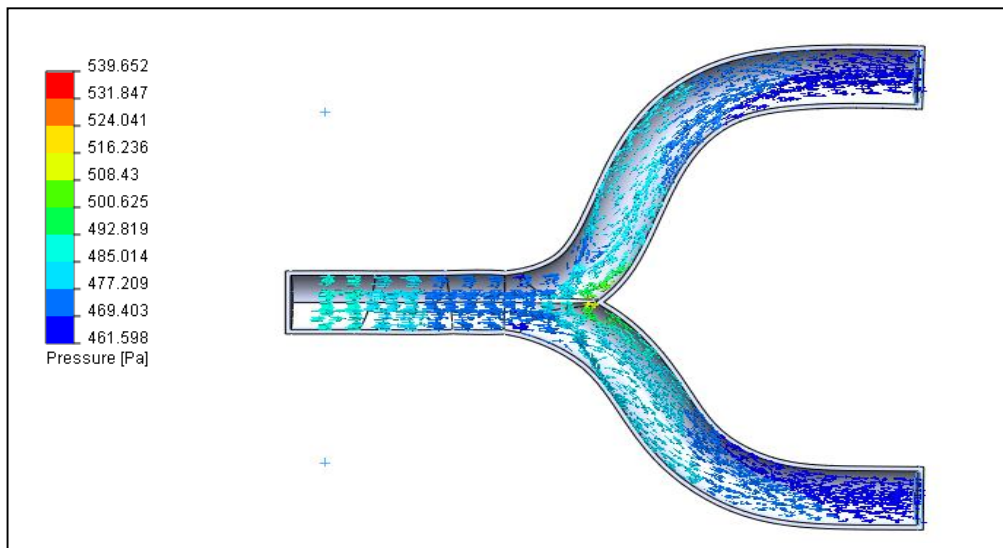


Figure 4.24 Pressure flow for normal microvessel bifurcations

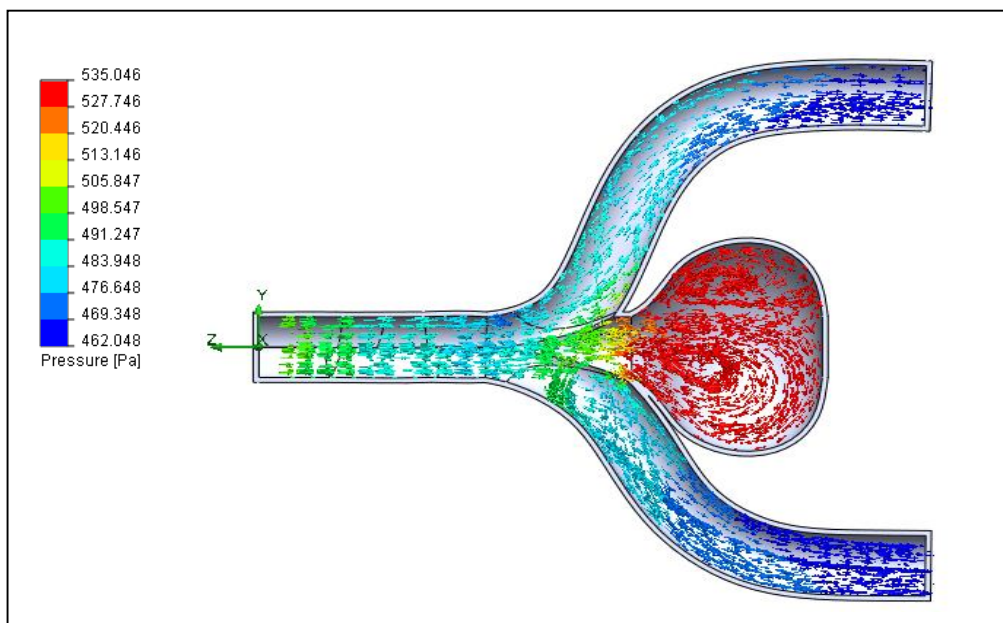


Figure 4.25 Pressure flow for abnormal microvessel bifurcations

For normal bifurcation model, the simulation shown the pressure increase after the blood pressure hit the wall at the bifurcation. Abnormal microvessel bifurcation model also shown a same result. Blood pressure reach the higher value when enter the aneurysm area.

This will proven the objectives of this study where bifurcation give an effect to the blood behavior. There a figures shown when change the diameter of blood vessel for normal and abnormal microvessel bifurcation. The entire figure showed an effect for every single model of microvessel bifurcation.

4.3.1 For normal microvessel bifurcations

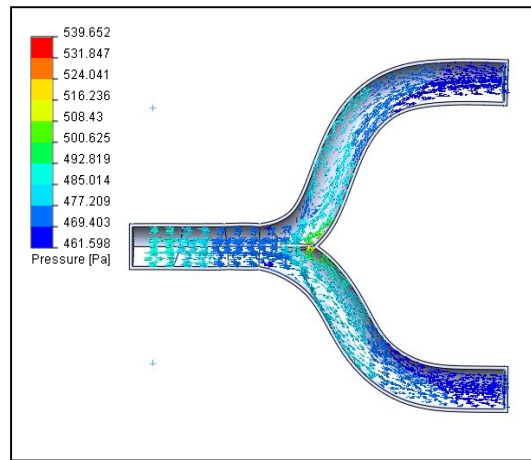
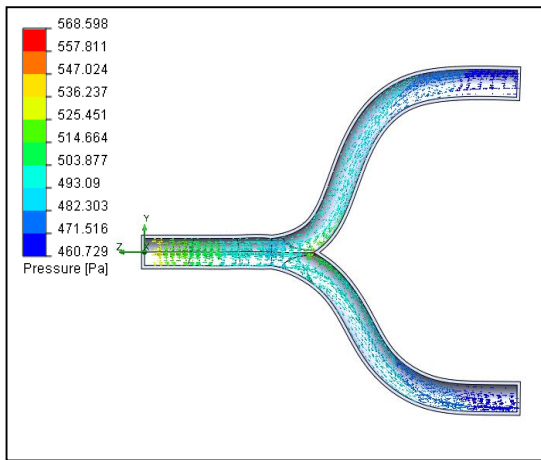


Figure 4.26 Pressure flow for diameter 5mm **Figure 4.27** Pressure flow for diameter 7mm

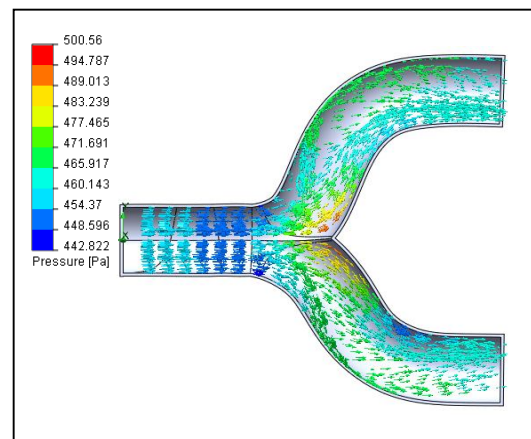
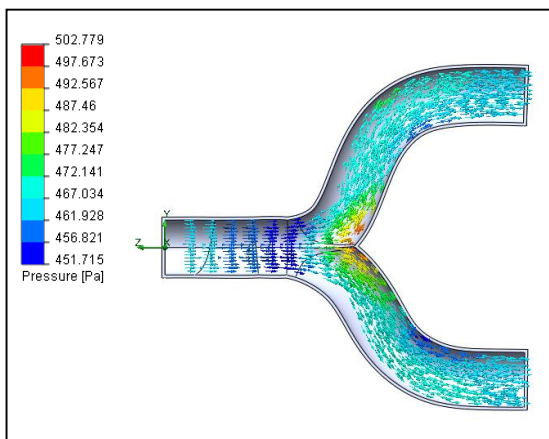


Figure4.28 Pressure flow for diameter 10mm **Figure4.29** Pressure flow for diameter 12mm

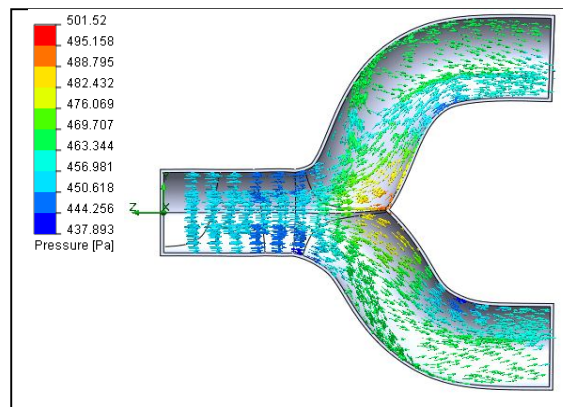


Figure 4.30 Pressure flow for diameter 14mm

4.3.2 For abnormal microvessel bifurcations

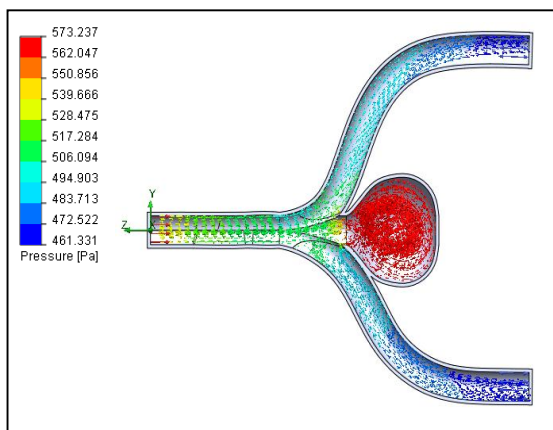


Figure 4.31 Pressure flow for diameter 5mm

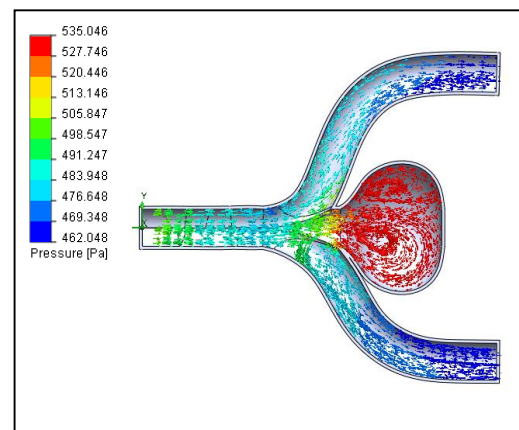


Figure 4.32 Pressure flow diameter 7mm

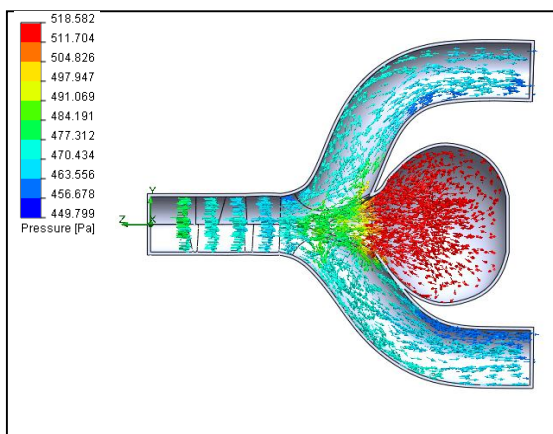


Figure 4.33 Pressure flow for diameter 10mm

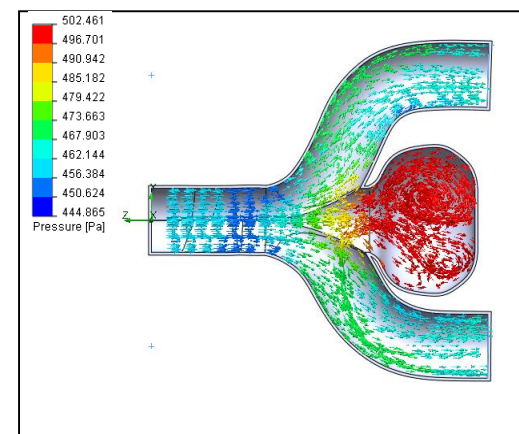


Figure 4.34 Pressure flow for diameter 12mm

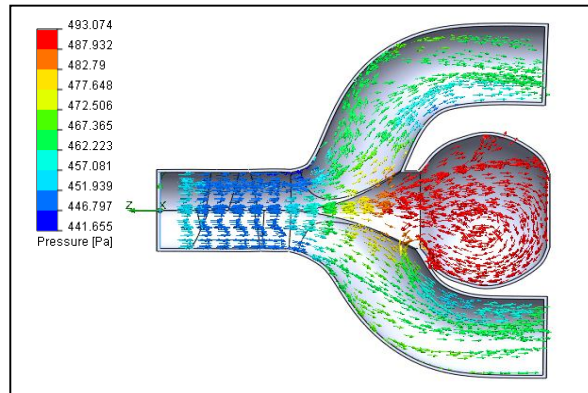


Figure 4.35 Pressure flow for diameter 14mm

4.4 REYNOLD'S NUMBER

$$\text{Reynold's number} = \frac{\rho V D}{\mu}$$

ρ = density of the blood

V = mean velocity blood (m/s)

μ = dynamic viscosity of blood (Pa.s/N/s/m²)

D = diameter of the blood vessel

Table 4.3 Change of blood vessel diameter

Diameter,mm	Reynold's number
5	496.875
7	695.625
10	993.75
12	1192.5
14	1391.25

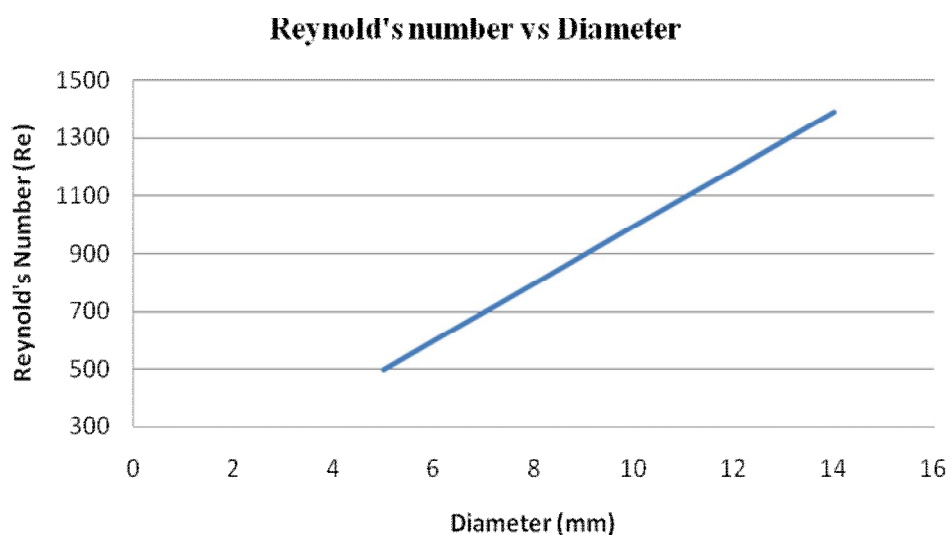


Figure 4.36 Graph Reynold's number vs diameter of blood vessel

When the diameter of blood vessel increased, the value for Reynold's Number also increased. From 5mm, Reynold's number value is 496.875 and increase when the diameter changes to 7mm. The value stay in increasing of Reynold's Number after diameter of blood vessel increase until 14mm. Blood flow in the blood vessel become more turbulent and the pattern of flow behavior at the bifurcation become not stable.

Table 4.4 Change velocity of the blood flow

Velocity,m/s	Reynold's number,Re
0.3	695.625
0.4	927.5
0.5	1159.375
0.6	1391.125
0.7	1623.125

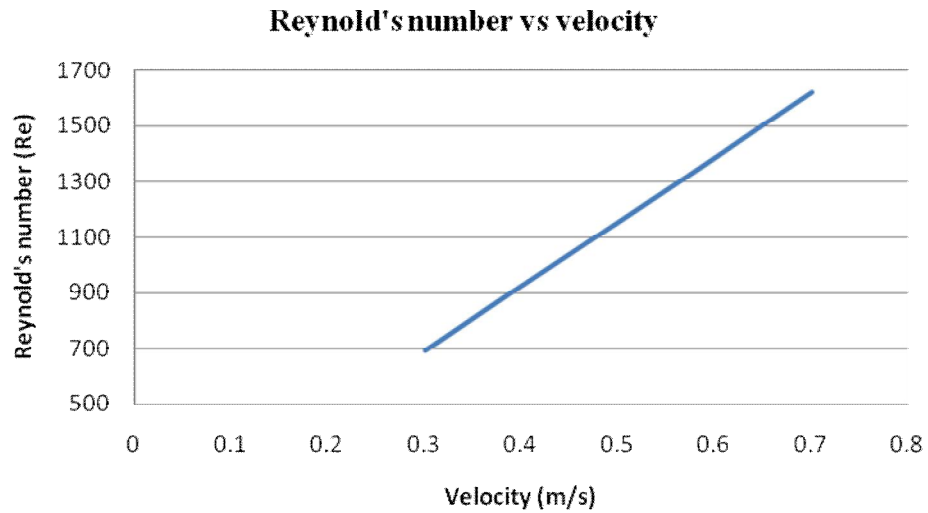


Figure 4.37 Graph Reynold's number vs velocity of blood vessel

When the velocity inlet gets an increment in values, the Reynold's Number are also increase. The lower the velocity, the smaller the value of Reynold's Number. This will leads to the blood flow become more laminar when the Reynold's Number decreases. For 0.3 m/s, the value of Reynold's Number is 695.625. Then, after increasing the velocity to 0.4 m/s, Reynold's number increase to 927.5. The continuity of this phenomenon happens until the last value of analysis which is 0.7 m/s.

Manual calculation on the Reynold's number :

For change in diameter of the blood vessel,

$$Re = \frac{\rho V D}{\mu}$$

Constant values :

$$\rho = 1060 \text{ kg/m}^3, \mu = 3.2 \times 10^{-3} \text{ Pa.s}, V = 0.3 \text{ m/s}$$

Diameter = 5mm

$$\text{Re} = \frac{\left(1060 \frac{\text{kg}}{\text{m}^3}\right) \left(\frac{0.3 \text{ m}}{\text{s}}\right) (5 \times 10^{-3} \text{ m})}{(3.2 \times 10^{-3} \text{ Pa.s})} = 496.875$$

Diameter = 7mm

$$\text{Re} = \frac{\left(1060 \frac{\text{kg}}{\text{m}^3}\right) \left(\frac{0.3 \text{ m}}{\text{s}}\right) (7 \times 10^{-3} \text{ m})}{(3.2 \times 10^{-3} \text{ Pa.s})} = 695.625$$

Diameter = 10mm

$$\text{Re} = \frac{\left(1060 \frac{\text{kg}}{\text{m}^3}\right) \left(\frac{0.3 \text{ m}}{\text{s}}\right) (10 \times 10^{-3} \text{ m})}{(3.2 \times 10^{-3} \text{ Pa.s})} = 993.75$$

Diameter = 12 mm

$$\text{Re} = \frac{\left(1060 \frac{\text{kg}}{\text{m}^3}\right) \left(\frac{0.3 \text{ m}}{\text{s}}\right) (12 \times 10^{-3} \text{ m})}{(3.2 \times 10^{-3} \text{ Pa.s})} = 1192.5$$

Diameter = 14mm

$$\text{Re} = \frac{\left(1060 \frac{\text{kg}}{\text{m}^3}\right) \left(\frac{0.3 \text{ m}}{\text{s}}\right) (14 \times 10^{-3} \text{ m})}{(3.2 \times 10^{-3} \text{ Pa.s})} = 1391.25$$

Change the velocity of the blood flow,

Constant values :

$$\rho = 1060 \text{ kg/m}^3, \mu = 3.2 \times 10^{-3} \text{ Pa.s}, D = 7 \text{ mm}$$

Velocity = 0.3m/s

$$\text{Re} = \frac{\left(1060 \frac{\text{kg}}{\text{m}^3}\right) \left(\frac{0.3\text{m}}{\text{s}}\right) (7 \times 10^{-3} \text{ m})}{(3.2 \times 10^{-3} \text{ Pa.s})} = 695.625$$

Velocity = 0.4m/s

$$\text{Re} = \frac{\left(1060 \frac{\text{kg}}{\text{m}^3}\right) \left(\frac{0.4\text{m}}{\text{s}}\right) (7 \times 10^{-3} \text{ m})}{(3.2 \times 10^{-3} \text{ Pa.s})} = 927.5$$

Velocity = 0.5m/s

$$\text{Re} = \frac{\left(1060 \frac{\text{kg}}{\text{m}^3}\right) \left(\frac{0.5\text{m}}{\text{s}}\right) (7 \times 10^{-3} \text{ m})}{(3.2 \times 10^{-3} \text{ Pa.s})} = 1159.375$$

Velocity = 0.6m/s

$$\text{Re} = \frac{\left(1060 \frac{\text{kg}}{\text{m}^3}\right) \left(\frac{0.6\text{m}}{\text{s}}\right) (7 \times 10^{-3} \text{ m})}{(3.2 \times 10^{-3} \text{ Pa.s})} = 1391.125$$

Velocity = 0.7m/s

$$\text{Re} = \frac{\left(1060 \frac{\text{kg}}{\text{m}^3}\right) \left(\frac{0.7\text{m}}{\text{s}}\right) (7 \times 10^{-3} \text{ m})}{(3.2 \times 10^{-3} \text{ Pa.s})} = 1623.125$$

Numerical simulation allows for the study of blood flow behavior that is difficult to measure directly in real aneurysm. Results from this CFD analysis provide detailed information on critical local flow parameters such as velocity and pressure near the aneuysm part. The correlation between the pressure, velocity and Reynold's number had been identified numerically.

CHAPTER 5

CONCLUSION AND RECOMMENDATIONS

5.1 CONCLUSION

The studies establish the correlation between diameter of the microvessel bifurcations and peak velocity for normal and abnormal case. For normal, the lowest peak velocity is from the diameter of 5 mm. The highest peak pressure results from the largest diameter. However, the different percentage of peak velocity between normal and abnormal velocity proved that the aneurysm give an effect to the blood flow at the branches.

The aneurysm effect can be seen from the velocity profile for different diameter of microvessel bifurcations. Normal case and abnormal case showed the different in result analysis. For normal case, the peak velocity percentage decrease like commonly. When the aneurysm added for abnormal case, the peak velocity percentage showed the different. The small percentages is at 5mm with 0.61% and the largest is for diameter 14mm with 33.9%.From the analysis, every single parameter will make an influences to the result analysis. Blood velocity and pressure are the main parameter to be clearly correct.

Finally, from these numerical results, this analysis satisfy the blood behavior at the branches will effect when aneurysm happen.

5.2 RECOMMENDATIONS

In order to obtain strong correlation between the stent structural void area and the best velocity bandwidth, the recommendations are as below:

1. Pulse may have effect on the rupture of aneurysms in their growth rate. Therefore, future studies should consider the pulsatile condition of blood flow simulation by introducing the different Reynolds number.
2. The aneurysms size may differ from case to case. So, by varying the aneurysms size this study will be able to predict the effect of dome size to the flow behavior.
3. Shear stress in the blood vessel also has an effect to the blood flow behavior. Therefore, the shear stress can be set as the new parameter must be considered in the study.
4. Temperature and vorticity of blood are constant in this study. The actual temperature and vorticity of blood must be use to get more accurate result.
5. Other parameters may have significant impact on flow vortices such as stent strut angle, strut thickness and stent shape design. The future studies may have these parameters to be studied.

REFERENCES

- P. Avolio: *Multi-branched model of the human arterial system*, Med. & Biol. Eng. & Computing, 1980, 709-718.
- AVOLIO, A. P., O'ROURKE, M. F., MANG, K., BASON, P. And Gow, B. S. (1976) *A comparative study of pulsatile arterial hemodynamics in rabbits and guinea pigs. Amer. J. Physiol.* 230.
- BAYLISS WM: *On the local reactions of the arterial wall to changes of internal pressure. J Physiol (Lond)*28:220-231, 1902.
- BharadvaJ BK, Mabon RF, Gliddens DP. *Steady flow in a model of the human carotid bifurcation: Part I Row visualization. J Biomech* 1982;15:349-362
- Burrowes KS, Hunter PJ, Tawhai MH. *Investigation of the relative effect of vascular branching structure and gravity on pulmonary arterial blood flow heterogeneity via an image-based computational model. Acad Radiol* 2005;12(11):1464–74.
- Chimowitz MJ, Weiss DG, Cohen SL, Starling MR, Hobson RW, for the Veteran's Affairs Cooperative Study Group 167. *Cardiac prognosis of patients with carotid stenosis and no history of coronary artery disease. Stroke.* 1994;25:759–765.
- Cutnell J, Johnson K. *Physics*. 4th ed. New York: Wiley; 1998.
- D.A. Steinman, C. Ross Ethier, X. Zhang and S.R. Karpik, *The effect of flow waveform on anastomotic wall shear stress patterns*, ASME Adv. Bioengng. (1995) 173-176.

- D.N. Ku and D.P. Giddens, *Laser Doppler anemometer measurements of pulsatile flow in a model carotid bifurcation*, J. Biomech.20(4) (1987) 407-421.
- D.N. Ku, D.P. Giddens, C.K. Zarins and S. Glagov, *Pulsatile Row and atherosclerosis in the human carotid bifurcation. Positive correlation between plaque location and low oscillating shear stress*, Arteriosclerosis 5 (1985) 293-302.
- Fung, Y.C., 1996, "*Biomechanics Circulation*," Springer, pp. 446-509.
- Gijzen FJH, van de Vosse FN, Janssen JD. *The influence of the non-Newtonian properties of blood on the flow in large arteries: steady flow in a carotid bifurcation model*. *Journal of Biomedics* 1999; **32**:601–608.
- Gupta SK, Khosla VK, Chhabra R, et al. *Internal carotid artery bifurcation aneurysms: surgical experience*. *Neurol Med Chir (Tokyo)* 2007;47:153–8.
- Jafari A, Zamankhan P, Mousavi SM, Kolari P. *Modeling of blood flow in microvessels*. In: *3rd European medical and biology engineering conference, Prague, Czech Republic; 2005*. ISSN: 1727-1983, Article No.: 1915.
- J. Bernsdorf, S.E. Harrison, S.M. Smith, P.V. Lawford, D.R. Hose, A lattice-Boltzmann HPC application in medical physics, in: M. Resch, Th. Bönisch, S. Tiyyagura, T. Furui, Y. Seo, W. Bez (Eds.), *High Performance Computing on Vector Systems 2006, Proceedings of the High Performance Computing Center Stuttgart, Springer, 2006, pp. 121_132*.
- K. Perktold, M. Resch and R. Peter, *Three-dimensional numerical analysis of pulsatile flow and wall shear stress in the carotid artery bifurcation*, J. Biomech. 24(6) (1991) 409-420.

- K. Perktold, R.O. Peter, M. Resch and Cl. Langs, *Pulsatile non-Newtonian flow in three-dimensional carotid bifurcation models: a numerical study of flow phenomena under different bifurcation angles*. *J. Biomedical Engng.* 13 (1991) 507-515.
- Ku, D.N., Giddens, D.P., Zarins, C.K., Glagov, S., 1985. *Pulsatile flow and atherosclerosis in the human carotid bifurcation positive correlation between plaque location and low oscillating shear stress*. *Arteriosclerosis* 5,293–302.
- Ku DN. *Blood flow in arteries*. *Annu Rev Fluid Mech* 1997;29:399–434.
- LeVeque, Randall (2002), *Finite Volume Methods for Hyperbolic Problems*, Cambridge University Press.
- Liesch D, Poll A, Moravec S: Flow studies in true-to-scale models of human renal arteries, in Yoshida Y, Yamaguchi T, Caro CG, Glagov S, Nerem RM (eds): *Role of Blood Flow in Atherogenesis*. Tokyo, Springer-Verlag Co, 1984, pp 91-96.
- Perktold K, Resch M. *Numerical flow studies in human carotid artery bifurcations: basic*. *J Biomed Eng.* 1990;12:111–123.
- Peskin CS, McQueen DM. 1989. *A three-dimensional computational method for blood flow in the heart. I. Immersed elastic fibers in a viscous incompressible fluid*. *J. Comput. Phys.* 81:372–405
- Pozrikidis C. *Modeling and simulation of capsules and biological cells*. Boca Raton, Florida: A CRC Press Company; 2003.

- R. Womersley, *Method for the calculation of velocity, rate of flow and viscous drag in arteries when the pressure gradient is known*, J.Physiol. 127 (1955) 553-563.
- Rodkiewicz CM, Sinha P, Kennedy JS. 1990. *On the application of a constitutive equation for whole blood*. J. Biomech. Eng. 112:198–206
- S.Q. Liu and Y.C. Fung, *Relationship between hypertension, hypertrophy, and opening angle of zero-stress state of arteries following aortic constriction*, J. Biomech. Engrg. I 11(4) (1989) 325-335.
- Rodkiewicz CM, Sinha P, Kennedy JS. 1990. *On the application of a constitutive equation for whole blood*. J. Biomech. Eng. 112:198–206
- Taylor, C. A., Hughes, T. Jr. and Zarins, C. K. *Finite element modeling of three-dimensional pulsatile flow in the abdominal aorta: relevance to atherosclerosis*, Annals of Biomedical Engineering, 1998, 26, 975-987.
- Toro, E. F. (1999), *Riemann Solvers and Numerical Methods for Fluid Dynamics*, Springer-Verlag.

APPENDICES A

Data collection of velocity:

Normal microvessel with different velocity

Length (m)	0.3m/s	0.4m/s	0.5m/s	0.6m/s	0.7m/s
0	0.3	0.4	0.5	0.6	0.7
0.001284995	0.303905501	0.403873341	0.503861506	0.603833804	0.703809192
0.00256999	0.304651037	0.404628652	0.504645237	0.60542075	0.70542595
0.005642201	0.31063796	0.410742213	0.511932293	0.612156015	0.713376906
0.011019654	0.323063656	0.424236739	0.527329636	0.628205571	0.730916233
0.016013004	0.333438429	0.43506578	0.536128783	0.636956007	0.738684233
0.020622249	0.341158363	0.454371014	0.554442422	0.654786191	0.751878466
0.028218061	0.352590434	0.459641655	0.559531557	0.658688058	0.755500881
0.028872611	0.35348417	0.462578072	0.561760671	0.660431583	0.758617875
0.033681778	0.3583576	0.461348214	0.558646903	0.65517725	0.759504188
0.037522816	0.36171659	0.453205827	0.545689138	0.63693203	0.751906151
0.040211543	0.361782063	0.439056411	0.524509253	0.607883382	0.727935319
0.04290027	0.35721534	0.418385283	0.495464119	0.569467614	0.690460469
0.045588996	0.348509871	0.404134555	0.476748255	0.546070515	0.642448469
0.048277723	0.335000609	0.393217613	0.462106321	0.537361308	0.614835764
0.049814138	0.321805668	0.381833512	0.446750215	0.508517696	0.604293211
0.050966449	0.310549585	0.354088176	0.412640968	0.468070594	0.568658149
0.052310813	0.290131633	0.314313595	0.365586838	0.412656953	0.521591048
0.053655176	0.259739541	0.259551095	0.301320814	0.338523525	0.460057887
0.054999539	0.21517848	0.205424522	0.238447889	0.268011485	0.380116664
0.056007812	0.169268982	0.187875081	0.218094379	0.24524796	0.304070596
0.056343903	0.154303396	0.17198243	0.199991237	0.225516666	0.279876943
0.056888765	0.140761505	0.166708331	0.194158574	0.21928712	0.256854515
0.057161197	0.136000952				0.250546514

Abnormal microvessel with different velocity

Length (m)	0.3m/s	0.4m/s	0.5m/s	0.6m/s	0.7m/s
0	0.3	0.4	0.5	0.6	0.7
0.000864978	0.301854008	0.401853473	0.502057999	0.602057552	0.703277284
0.001946322	0.302629097	0.403295629	0.50329581	0.603297066	0.706765913
0.002354249	0.303308471	0.406756505	0.506772997	0.606785558	0.712116703
0.004116542	0.306759931	0.41188935	0.511995264	0.612080523	0.718044157
0.005983751	0.311801947	0.417294718	0.517589513	0.617855083	0.725009404
0.007820577	0.317055397	0.423408709	0.524000324	0.624538229	0.731366369
0.009969077	0.322988933	0.429001268	0.529830076	0.630620201	0.736801239
0.012074689	0.328428581	0.434009622	0.534949378	0.635902195	0.741074584
0.014145903	0.333267334	0.43821894	0.539189164	0.640176866	0.744869769
0.016102177	0.337256484	0.442092528	0.543086186	0.644053473	0.748218968
0.018111576	0.340820206	0.445428186	0.546509172	0.647459555	0.751589997
0.019994346	0.343780555	0.448556537	0.549833578	0.650814724	0.755162958
0.02185465	0.346479856	0.451600525	0.553189366	0.654290991	0.759068998
0.023693016	0.349046895	0.454653894	0.556686858	0.658003827	0.762869649
0.025509957	0.351569852	0.457459904	0.559999991	0.661540545	0.766355302
0.027205409	0.353883731	0.460036733	0.563042377	0.664800549	0.769059137
0.028956691	0.356083699	0.462227944	0.565502041	0.66746401	0.770569817
0.03086612	0.358050706	0.463900764	0.567097684	0.669142653	0.771210806
0.032978209	0.359666334	0.465057024	0.567989077	0.669970795	0.771544899
0.035001674	0.360987304	0.465997239	0.568657969	0.670437998	0.771245708
0.037170658	0.362370874	0.466040792	0.568547636	0.670216354	0.769132634
0.038698673	0.363039448	0.465488013	0.567625223	0.668604985	0.768210043
0.0391115149	0.362884111	0.462871206	0.567088742	0.667856887	0.762675966
0.040775703	0.361999479	0.462015565	0.562788561	0.663374001	0.758636714
0.041045698	0.361567902	0.4566838	0.561501905	0.660111614	0.745039428
0.042615577	0.358825741	0.455366441	0.553560003	0.649178346	0.741752203
0.04288701	0.358077567	0.446328279	0.551680469	0.646571799	0.719607247
0.044640057	0.352963936	0.435015334	0.539009538	0.628953328	0.694152243
0.046384139	0.346598573	0.422919701	0.524209023	0.608254258	0.661597703
0.048215533	0.338493779	0.417567806	0.506624837	0.583827974	0.629815489
0.04847789	0.337078881	0.40192534	0.503765183	0.579936785	0.59800801
0.050224757	0.327212495	0.39657574	0.486596962	0.556767048	0.567865025
0.050460326	0.325695198	0.37418659	0.480595263	0.548962598	0.545696455
0.052421731	0.313514755	0.362653636	0.461041453	0.518959222	0.530397529
0.053486671	0.307268704	0.358840598	0.452998255	0.513945018	0.515872367
0.054275686	0.305220002	0.353725293	0.425190197	0.494010144	0.481340804
0.055335171	0.302474711	0.355621727	0.409762264	0.482154287	0.463574966
0.05640859	0.302176637	0.35701695	0.399615434	0.450226069	0.403422667
0.05718367	0.301995901	0.353443298	0.392336552	0.438524266	0.381310943
0.058400062	0.295612843	0.351617851	0.385913638	0.398203241	0.297329488
0.05903217	0.292354432	0.329980552	0.383136574	0.377326011	0.266705729
0.06038216	0.271451525	0.322024987	0.365742588	0.30163684	0.176646875
0.06088067	0.263784629	0.282620509	0.359725939	0.274441832	0.139544048
0.062233288	0.229409562	0.26818519	0.314622907	0.206420793	0.089634964
0.062729169	0.216831655	0.212834087	0.298168846	0.191775285	0.059494962
0.064026527	0.171772083	0.189331872	0.234249059	0.163628892	0.033817496
0.065433802	0.122034789	0.138469375	0.186922872	0.11765611	0.0267697
0.065681894	0.113178537	0.104397484	0.155079441	0.106056094	0.022330031
0.066426169	0.086661643	0.063202941	0.120153944	0.084824008	0.021009594
0.068210106	0.053514829	0.035260825	0.079601718	0.067238493	0.020964017
0.070123168	0.021273642	0.023490599	0.054952504	0.055983843	0.021074866
0.072328272	0.016988873	0.016957785	0.043799307	0.054647338	0.014726806
0.074674872	0.013279918	0.01279063	0.036632767	0.054883335	0.010822069
0.07634166	0.011342431	0.012360742	0.025030387	0.056956632	0.007045003
0.081214166	0.005845974	0.012441707	0.016967071	0.054280057	0.007119173
0.084401961	0.005220176	0.007306216	0.015779865	0.052802282	0.016062305
0.090114653	0.003754941	0.006212955	0.016678617	0.035669727	0.0172474
0.091514373	0.003774989	0.005689675	0.017948291	0.030471266	0.016999758
0.092305165	0.003804155	0.007349046	0.017527641	0.027359545	0.016423691
0.096002164	0.002907214	0.008607702	0.017522792	0.020076813	0.014081342
0.098057417	0.002248036	0.010723102	0.017530656	0.017617683	2.1684E-19
0.099651666	4.47028E-19	0.010618686	0.012932807	0.015335413	0
0.099651667	0	0.009294651	0.010722862	0.014380169	
		1.73472E-18		0.014772788	
		0		0.015680104	
				0.027043174	
				0.031239881	
				0.034007501	
				0.031968675	
				3.46945E-18	
				0	

Normal microvessel with different diameter

Length (m)	5mm	7mm	10mm	12mm	14mm
0	0.3	0.3	0.3	0.3	0.3
0.000556102	0.301671694	0.303905501	0.301930154	0.301028551	0.300838603
0.000929084	0.301957445	0.304651037	0.302897373	0.30154958	0.301345685
0.001819943	0.304368943	0.31063796	0.303406151	0.30274411	0.302682047
0.002343826	0.30640349	0.323063656	0.306638035	0.305276933	0.304850587
0.002607708	0.307570649	0.333438429	0.307276125	0.308147349	0.307184143
0.003389761	0.311253687	0.341158363	0.312016225	0.310790745	0.309528925
0.004095674	0.314828274	0.352590434	0.316278849	0.313490995	0.312009838
0.00492611	0.319032212	0.35348417	0.319858617	0.315882173	0.315046828
0.005699351	0.322811755	0.3583576	0.323373759	0.318139325	0.314662963
0.006454258	0.326380043	0.36171659	0.326572119	0.320045658	0.313570983
0.007922411	0.332903818	0.361782063	0.329850158	0.321396321	0.309097597
0.009294846	0.338686799	0.35721534	0.333013049	0.321900617	0.298017564
0.010743919	0.34455539	0.348509871	0.335013846	0.321964805	0.287165496
0.012084977	0.349812699	0.335000609	0.335699127	0.320613492	0.262453852
0.013351273	0.354582471	0.321805668	0.335182198	0.31944348	0.249237884
0.014568214	0.358916642	0.310549585	0.334399168	0.316595938	0.237096496
0.015709178	0.362713547	0.290131633	0.331646523	0.315169499	0.219812317
0.017011351	0.366710835	0.259739541	0.328982891	0.308651712	0.207037914
0.018160561	0.369990112	0.21517848	0.323103321	0.30462397	0.186452583
0.019257576	0.372917877	0.169268982	0.318635842	0.292214717	0.171788675
0.020325808	0.375603127	0.154303396	0.307955027	0.268491586	0.140994222
0.021366157	0.378084387	0.140761505	0.303502961	0.250990504	0.130583571
0.022379494	0.380401332	0.136000952	0.286720753	0.214070182	0.096932017
0.023343642	0.382546432		0.283392193	0.196620787	0.08539657
0.024155363	0.384331316		0.260228711	0.175671142	0.074700359
0.025211136	0.386667518		0.257038378	0.150087161	
0.026055982	0.388588175		0.220805711	0.128751393	
0.026936574	0.390636579		0.173015133	0.11414813	
0.027786437	0.392625912		0.158284728	0.057329895	
0.028598931	0.394488294		0.130164504	0.014462764	
0.029328364	0.39606842		0.068323902		
0.030105703	0.397520746		0.028985491		
0.031545774	0.399712673		0.028849182		
0.032953046	0.401169273		0.026916214		
0.034251806	0.402392324				
0.035458641	0.403761479				
0.036563994	0.405345004				
0.037622258	0.407102989				
0.038636375	0.408761761				
0.039561249	0.40983528				
0.039991959	0.410242368				
0.040442096	0.41009963				
0.041047732	0.409907587				
0.041262591	0.408929454				
0.041989965	0.405618149				
0.042103505	0.405101271				
0.04307278	0.389886107				
0.043315099	0.387069098				
0.043615083	0.384259832				
0.044215051	0.378641355				
0.045787578	0.368312646				
0.046888307	0.361437536				
0.047169162	0.359771472				
0.047450017	0.359159948				
0.047966629	0.364148797				
0.048438143	0.368702165				
0.049493916	0.356118911				
0.049991118	0.345770161				
0.05054969	0.334145487				
0.051025194	0.31739345				
0.051605463	0.29695753				
0.052360836	0.253858323				
0.052661236	0.236785118				
0.052971634	0.224820651				
0.053385814	0.20893255				

Abnormal microvessel with different diameter

Length (m)	5mm	7mm	10mm	12mm	14mm
	0	0.3	0.3	0.3	0.3
0.000666163	0.30317329	0.30185346	0.30121027	0.301304984	0.300967016
0.001387513	0.304241008	0.302628563	0.301865903	0.302126053	0.301689883
0.001728971	0.30560418	0.30330785	0.303751803	0.304102627	0.30339428
0.002810309	0.309921181	0.306758929	0.307320591	0.305057486	0.306114887
0.004288291	0.318043132	0.311801413	0.311160506	0.308737302	0.308993819
0.005593798	0.324778503	0.317057778	0.314811149	0.312527608	0.311598647
0.006897617	0.330639916	0.322994283	0.318029971	0.31602163	0.313089963
0.008185662	0.335754097	0.328432833	0.321123072	0.31883225	0.3133204
0.009455437	0.340334782	0.333269696	0.323870355	0.319899743	0.312208517
0.01070632	0.344536119	0.337257884	0.326460809	0.320180417	0.311227149
0.011935632	0.348430186	0.340820622	0.329101052	0.320320024	0.306431709
0.01304849	0.351754857	0.343780315	0.331402823	0.317631363	0.293959905
0.014295026	0.35511757	0.346483467	0.333920752	0.316897381	0.27385343
0.015497072	0.358042655	0.349052362	0.335655518	0.308653305	0.267435994
0.01662828	0.360550123	0.35156983	0.336913156	0.306924911	0.247801977
0.017592855	0.362545583	0.353883038	0.337508891	0.290112075	0.237841954
0.018877316	0.364948936	0.356087551	0.337557902	0.269147922	0.204731512
0.019971654	0.366894686	0.358059075	0.336706672	0.246627525	0.183531609
0.02103444	0.368738184	0.35967724	0.335465091	0.224071818	0.171818349
0.022027823	0.370433532	0.360996424	0.333757386	0.197656081	0.159169317
0.023144812	0.372307676	0.36237808	0.332960361	0.188953373	0.14673479
0.024191168	0.374070551	0.36304919	0.326598493	0.159171937	0.138763916
0.025204829	0.375805129	0.36289417	0.325524268	0.150488205	0.127120361
0.026155778	0.377509427	0.362010356	0.314094824	0.124745841	0.122492498
0.027175022	0.379401178	0.361578585	0.301995113	0.111871561	0.105921674
0.028153138	0.381207382	0.358833109	0.292483662	0.095942397	0.098006324
0.029419436	0.383376656	0.358082286	0.286710538	0.085771628	0.07966042
0.030897759	0.385299731	0.352948531	0.284640484	0.063888299	0.051530497
0.032252298	0.386485655	0.346560639	0.283899462	0.054931014	0.03201176
0.033655588	0.387412637	0.338455013	0.279585408	0.037366787	0.020583278
0.034946841	0.388396995	0.337039416	0.277379666	0.030704209	0.015639278
0.036626957	0.39025789	0.327167828	0.270049157	0.023348691	0.010138322
0.038184212	0.392569736	0.325649685	0.263513375	0.016603808	0.009650426
0.039767695	0.394308738	0.313470014	0.199791155	0.013679579	0.009473876
0.041246018	0.393657181	0.307230644	0.19130479	0.016323337	0.010013714
0.04272434	0.390602304	0.305192064	0.100637658	0.011682751	0.009978242
0.044202663	0.386125471	0.302461106	0.034739406	0.006909695	1.80121E-18
0.045680986	0.380894373	0.302221545	0.018847086	0.006220508	4.33681E-19
0.04701797	0.375655646	0.30206616	0.012257071	0.005814018	
0.048337053	0.370178408	0.295800672	0.003274956	0.004258374	
0.049620953	0.364841425	0.292600343	0.002122566	0	
0.05086724	0.360482105	0.271763365	0.001878459		
0.052068899	0.35683777	0.264117752	0.003616209		
0.053072599	0.353868245	0.229473749	0.003777836		
0.054349607	0.342906007	0.216797708	0.004589975		
0.054550922	0.341189269	0.172419887	0.004243829		
0.055430699	0.324777035	0.114861641	0.002659728		
0.056029244	0.313655977	0.088841629	4.37266E-19		
0.056483489	0.300505955	0.055724426			
0.057402036	0.27415581	0.022945501			
0.057507567	0.271152345	0.018127681			
0.058457233	0.236377445	0.014987947			
0.05898589	0.217352894	0.011954939			
0.059899776	0.180926275	0.006421994			
0.061248657	0.12924564	0.00583637			
0.061942535	0.104119094	0.004684611			
0.062795553	0.080583198	0.004683127			
0.063216278	0.069194764	0.004685005			
0.063637004	0.060104851	0.0046968			
0.064478455	0.046647575	0.003412024			
0.06489918	0.040584083	0.00261708			
0.065912835	0.034400369	0			
0.068023257	0.021813416	0			
0.068394285	0.020180939				
0.070812471	0.009682544				
0.074277294	0.005459788				
0.076725762	0.001642746				
0.077475122	0.001567105				
0.079706883	0.001950635				
0.082639053	0.003439322				
0.085048611	0.002963678				
0.087870468	0.001954264				
0.08852343	0.001684128				
0.088800833	0				

APPENDICES B

Data collection for pressure:

Normal microvessel with different velocity

Length (m)	0.3 m/s	0.4m/s	0.5m/s	0.6m/s	0.7m/s
0	492.6789601	493.05533	487.0593199	474.8167644	456.2158016
0.00256999	491.6861216	491.7327922	485.3962467	472.8224271	453.8962142
0.007178616	488.2486679	486.7106676	479.4968897	466.2144533	446.0242235
0.014476589	482.9308974	480.8566637	473.3909482	457.9919637	436.0443579
0.017165315	481.1324566	477.8968362	468.4999117	452.5864892	430.0666714
0.023310976	477.4382781	469.1233868	460.1794614	443.1542624	419.559556
0.028872611	474.1622402	468.8972947	457.474645	439.6216937	415.1017566
0.030224844	473.4737348	468.0137136	456.4546255	438.545713	414.0057376
0.032529467	472.461254	466.78269	455.1267153	437.3127947	412.948438
0.037522816	470.7092787	464.8606296	453.4766657	436.303125	412.758291
0.040211543	470.3982822	464.9682863	454.4511614	438.5583271	412.799105
0.04290027	471.7214654	468.303859	460.9921556	449.5073681	416.9089243
0.045588996	474.7079547	474.7238984	472.6582917	468.1744178	433.541718
0.048277723	479.0154679	483.112688	486.857434	489.9958595	460.9617544
0.049430034	481.7469194	487.9928078	494.538315	501.1415593	492.1454445
0.049814138	482.9379037	490.0684495	497.7603978	505.7553884	507.1878536
0.050966449	487.3523582	497.6421797	523.1257361	524.934206	513.4024777
0.052310813	493.215035	507.1233291	539.6237603	540.7834653	535.6478135
0.053655176	500.8748074	519.1533978	556.8223098	567.6750457	559.6272483
0.054999539	509.2960029	531.9776117	570.9373382	584.1622681	613.6706322
0.056343903	516.5453447	542.5336614	569.3654812	602.3056151	635.5263811
0.056888765	515.8700448	541.3849534	567.7246292	600.2358375	632.8123575
0.057161197	515.1832981	540.2167381		598.288012	629.9625562

Abnormal microvessel with different velocity

Length (m)	0.3m/s	0.4m/s	0.5m/s	0.6m/s	0.7m/s
0	503.2218699	508.0120982	508.7594474	507.9304513	502.305666
0.001729956	502.7377954	507.1904633	507.7291917	506.6911359	500.8660892
0.002354249	502.363076	506.8648216	507.3211609	506.1990229	500.2939649
0.003854629	501.4092652	505.5942699	505.377205	503.8548058	497.5608839
0.004116542	501.2016693	505.3162452	502.7489956	500.6683288	493.8109788
0.005983751	499.6584801	503.2394162	499.8626145	497.1085308	489.5649187
0.007820577	498.003001	500.9895636	496.5476291	492.9740907	484.5601314
0.009969077	496.1177131	498.4348739	493.4731723	489.1751567	479.9425832
0.012074689	494.3556965	496.0644551	490.7199881	485.8058755	475.9191867
0.014145903	492.7459009	493.8968768	488.4262169	483.0522668	472.7431795
0.016102177	491.3935276	492.0441686	486.3161903	480.5618232	469.9319407
0.018111576	490.1683029	490.3256926	484.456579	478.3636713	467.4176296
0.019994346	489.1333799	488.8315159	482.638412	476.185908	464.8637602
0.02185466	488.1766024	487.4184813	480.7923117	473.9135894	462.1491565
0.023693016	487.2611609	486.0400755	478.8752263	471.4947184	459.2389775
0.025509957	486.3545279	484.652999	477.0300478	469.152441	456.4085115
0.027205409	485.5108599	483.3579095	475.2963502	466.970933	453.7921317
0.028956691	484.6965632	482.1399549	473.8547872	465.1896507	451.7239232
0.03086612	483.9359508	481.0857972	472.882659	464.1083496	450.5809428
0.032978209	483.2796049	480.2861545	472.3446267	463.6605509	450.2330455
0.035001674	482.7861004	479.7440519	472.0055757	463.4595056	450.076668
0.037170658	482.2978785	479.3052936	472.0616286	463.5971459	450.2736635
0.038698673	482.0434035	479.2396831	472.3285047	464.2528388	451.2123697
0.039115149	482.0760879	479.4597168	472.8295001	465.0742493	452.3766458
0.040547173	482.1882617	480.2159708	474.5516934	467.8979424	456.379273
0.041045698	482.4402204	480.9083571	475.8965955	470.0454437	459.3777891
0.042395673	483.1223575	482.783079	479.5381879	475.8602621	467.4971549
0.04288701	483.5915769	483.8620697	481.4833362	478.9834615	471.8125205
0.044397955	485.0800308	487.270109	487.5758236	488.7606451	485.290765
0.044640057	485.3829704	487.9433948	488.708783	490.571818	487.7441987
0.046384139	487.6235824	492.0874044	496.9983437	503.7731162	505.4891537
0.047941172	489.8828906	492.9328813	506.5107879	520.7630212	527.1450435
0.04847789	490.7948412	498.005914	507.9871762	537.5605721	547.233121
0.050007214	493.4389011	500.0708541	516.6899803	549.6678667	561.2468697
0.050460326	494.3034762	505.1177697	519.4412588	553.7497742	566.0051165
0.051896834	496.9929163	508.0019698	531.1714913	562.0311293	575.6585509
0.052421731	497.8898056	513.0672892	537.394051	566.3636587	581.7703893
0.053486671	499.7094867	516.0210556	540.7792762	572.1813075	589.9773495
0.054275686	500.3016637	520.0354024	545.3248206	573.2438255	595.9705907
0.055335171	501.0969225	521.2962735	546.3321467	574.0115736	607.1226631
0.05640859	500.8383768	522.9893273	547.0597728	571.5936204	610.6696188
0.05718367	500.6518675	521.9752778	544.5438864	570.3379498	622.4111982
0.058400062	500.6842294	521.2433109	543.2370521	571.8135763	626.747573
0.05903217	500.7012729	518.3566922	545.0586558	572.3590565	643.7781022
0.06038216	503.4884886	516.8570835	545.7316901	582.6287658	653.6085294
0.06088067	504.517839	517.38998	554.4801307	586.3938111	668.2378342
0.062233288	510.7271415	517.5869743	557.6874369	602.0297155	675.9761146
0.062729169	513.0034506	525.6392474	568.6315265	608.671768	685.925619
0.064026527	519.91083	528.5911375	573.2805717	619.3761728	692.6314649
0.064577669	522.8449881	539.3146582	581.1001997	626.5907542	698.1509245
0.065681894	526.8059121	543.8698874	586.3705929	633.7071284	703.9198765
0.066426169	529.4755407	550.314825	591.4214025	641.1752808	705.4448262
0.068210106	531.6887614	554.6587474	596.6807857	643.1317924	706.4764697
0.070123168	533.933077	558.1619804	597.8867053	644.4554463	706.7020172
0.072328272	534.3325766	561.7280501	598.7025496	644.7793352	707.1535205
0.073820168	534.6028801	562.2564125	598.9447497	645.4466542	707.3397715
0.07634166	534.7662659	562.613921	599.3643783	645.6576156	707.5123634
0.082282288	535.0381083	562.7756973	599.3726376	645.9036864	707.5689695
0.084401961	535.0495301	563.0763929	599.4835009	646.0051331	707.5689695
0.091514373	535.0837708	563.0855718	599.695505	646.0051332	
0.096002164	535.0936017	563.0897429	599.7943331		
0.099651666	535.0970771	563.088165	599.7943331		
0.099651667	535.0970771	563.139515			
		563.2085274			
		563.2321298			
		563.2321298			

Normal microvessel with different diameter

Length (m)	5mm	7mm	10mm	12mm	14mm
0	532.1190623	492.6789601	467.4354862	459.048714	454.0781376
0.000929084	531.6964814	491.6861216	466.962747	458.7952121	453.8410001
0.001819943	530.8487895	488.2486679	466.5691751	458.6610708	453.7382641
0.002224088	530.3759686	482.9308974	465.6548813	458.2333355	453.2908021
0.002607708	529.86955	481.1324566	465.274437	457.4710487	452.640691
0.003259223	528.953434	477.4382781	463.7968436	456.5854395	451.9323134
0.003389761	528.7477142	474.1622402	462.8249805	455.7691513	451.2681502
0.004095674	527.6352388	473.4737348	462.4515766	454.9295737	450.7928641
0.00492611	526.3111988	472.461254	461.3200345	454.183318	450.6851503
0.005699351	525.1076849	470.7092787	460.1802278	453.491744	450.0416973
0.006454258	523.9599058	470.3982822	459.1389998	452.9126789	450.1555772
0.007922411	521.8209477	471.7214654	458.0708509	452.5194568	450.4803713
0.009294846	519.8853532	474.7079547	457.0249226	452.4319259	451.5801866
0.010743919	517.8761051	479.0154679	456.4974255	452.4164439	454.306448
0.012084977	516.0415524	481.7469194	456.4020892	452.4107966	457.1182952
0.013351273	514.3466096	482.9379037	456.2131482	452.8372613	463.5495536
0.014568214	512.7762145	487.3523582	456.3402706	452.9820417	466.8854488
0.015709178	511.3773574	493.215035	456.532792	454.160286	473.6600486
0.017011351	509.8766364	500.8748074	457.3704988	454.6327198	477.0803839
0.018160561	508.6235365	509.2960029	458.1811313	456.5872966	479.956154
0.019257576	507.486955	516.5453447	460.0997123	457.795355	482.4888813
0.020325808	506.4277809	515.8700448	461.557523	461.019958	486.6046543
0.021366157	505.4336572	515.1832981	464.8559504	467.2308086	488.0186001
0.022379494	504.4920252		466.2307967	471.1490939	490.8865813
0.023343642	503.6093314		471.0228618	479.4601601	491.8820462
0.024155363	502.8675461		471.9734514	482.6549241	491.6745636
0.025211136	501.8871702		478.0055802	486.4961211	
0.026055982	501.0776826		478.8366685	489.8604595	
0.026936574	500.2117295		486.5649012	492.6745404	
0.027786437	499.3641709		494.027054	493.7350756	
0.028598931	498.5605351		495.48568	494.5840309	
0.029328364	497.8648274		496.2844879	495.2011366	
0.030105703	497.204457		497.188518		
0.031440617	496.2346369		497.9869757		
0.031545774	496.1627709		497.5463436		
0.032953046	495.4035101		497.5385699		
0.034251806	494.7551337				
0.035458641	494.0646434				
0.036563994	493.2852781				
0.037622258	492.4492658				
0.038636375	491.6561547				
0.039176932	491.3015884				
0.039561249	491.1059923				
0.039991959	490.8867846				
0.040442096	490.8474655				
0.041047732	490.7945638				
0.041262591	490.8799807				
0.041989965	491.1691463				
0.042103505	491.2142837				
0.043615083	492.6807056				
0.044215051	493.2990133				
0.045787578	495.4282739				
0.046326597	496.1581015				
0.047169162	497.6763753				
0.047450017	498.2474792				
0.047966629	499.674895				
0.048438143	500.9777045				
0.049493916	505.0929126				
0.049991118	508.3386185				
0.05054969	511.984944				
0.051025194	516.1708857				
0.051605463	521.2790797				
0.052360836	528.5106691				
0.052661236	531.3865491				
0.052971634	531.4568511				
0.053385814	531.5506588				

Abnormal microvessel with different diameter

Length (m)	5mm	7mm	10mm	12mm	14mm
	0				
0.001387513	542.0185996	503.1975873	480.5429828	461.0736116	453.2863628
0.001728971	541.5348886	502.3387598	480.2068824	460.6992349	452.9921564
0.002810309	540.0030618	501.3848625	479.42463	459.8600615	452.2794151
0.004288291	537.4345413	501.1772535	478.3524703	459.574194	451.4595935
0.005593798	535.2350113	499.6340029	477.1704391	458.4546764	450.610726
0.006897617	533.2784734	497.9785152	476.0364589	457.275532	449.8649223
0.008185662	531.5383069	496.0931641	475.0262983	456.1768226	449.6523556
0.009455437	529.9420754	494.3311523	474.0443427	455.597046	449.467021
0.01070632	528.4483486	492.7214612	473.1640169	455.3071266	449.4084064
0.011935632	527.0416364	491.3691741	472.330401	455.0262058	449.7145659
0.01304849	525.8106812	490.143967	471.4770125	454.9467759	449.7520186
0.014295026	524.5249916	489.1092113	470.7285108	454.9204833	451.3834463
0.015497072	523.3799281	488.1527653	469.8981583	455.6945651	454.9880389
0.01662828	522.3769159	487.2371171	469.3235518	455.9059249	460.5622087
0.017592855	521.5651633	486.3294243	468.9196197	458.2785014	462.2143702
0.018877316	520.5600914	485.4841116	468.7556398	458.7762575	469.5108795
0.019971654	519.7286744	484.6680631	468.7562441	463.7381579	474.0176023
0.02103444	518.9302945	483.9065003	468.8140883	469.5667068	476.6572557
0.022027823	518.1883526	483.2505231	469.0496296	475.2161797	480.0956832
0.023144812	517.3474116	482.7575755	469.1765098	480.5875215	482.7284192
0.024191168	516.5521656	482.2701106	470.0170394	486.9107861	484.8836278
0.025204829	515.7706679	482.0166122	470.2767154	491.0981835	486.7237489
0.026155778	515.0129393	482.0495549	472.0262453	492.1891911	487.9055563
0.027175022	514.1653323	482.1626179	474.6064468	495.4622139	488.6697556
0.028153138	513.3435331	482.4148417	477.4552063	496.9115771	489.0623765
0.029419436	512.3089596	483.097697	480.5429797	498.7295828	489.4887558
0.030897759	511.3189193	483.5670686	482.4209894	499.4955109	489.7903224
0.032252298	510.6245893	485.0561655	482.0232454	500.27097	490.6863989
0.033655588	510.0110085	485.3594544	481.8776954	500.6308499	491.644262
0.034946841	509.4105616	487.6030865	481.3017527	500.9100904	492.0936905
0.036626957	508.4210015	489.867329	481.2177531	501.083433	492.3376004
0.038184212	507.2941633	490.7815537	481.5364492	501.3616905	492.4876021
0.039767695	506.3284192	493.4324567	481.8206543	501.3808159	492.6105163
0.041246018	506.1657323	494.2997097	491.4642574	501.4735106	492.678429
0.04272434	506.9915559	496.9983093	492.7497221	501.5763265	492.6785408
0.044202663	508.4207114	497.8996601	508.0555198	501.61217	
0.045680986	509.9199283	499.7283918	515.3768563		
0.04701797	511.1374714	500.3278993	516.7880461		
0.048337053	512.0505596	501.1330006	517.1339159		
0.049046792	512.368855	500.8761778	517.1474996		
0.049620953	512.5345953	500.6909136	517.1860498		
0.050115954	512.6774847	500.7168407	517.2048871		
0.05086724	512.589369	500.7305408	517.2094581		
0.052068899	512.4284323	503.5016446	517.2101759		
0.053072599	512.268421	504.5250442			
0.054349607	514.2848313	510.7136046			
0.054550922	514.6027097	512.9823069			
0.055430699	518.9875765	519.8876786			
0.056029244	521.9707639	522.8209776			
0.056483489	525.7179456	526.7573997			
0.057402036	533.2952659	529.4105148			
0.057894291	537.6661893	531.580341			
0.058457233	542.761574	533.7740715			
0.05898589	547.5466225	534.1781659			
0.059899776	554.6224951	534.4515775			
0.060464212	558.9927055	534.6148457			
0.061248657	563.0744225	534.8881824			
0.061942535	566.684893	534.9014956			
0.062795553	568.2290554	534.9435941			
0.06489918	572.0005974	534.9558126			
0.065912835	572.1885047	534.9594444			
0.068394285	572.5784021	534.9594444			
0.070812471	572.7118437				
0.073461138	572.7187373				
0.074277294	572.7167048				
0.076725762	572.70305				
0.079706883	572.7139088				
0.085048611	572.727367				
0.087870468	572.731378				
0.088552343	572.7321413				
0.088800833	572.7297446				